Modulators of proteostasis: therapeutic targets and diagnostic markers to halt and reverse atrial fibrillation

Marion, D.M.S.

2021

document version
Publisher's PDF, also known as Version of record

Chapter 7

Screening of novel HSP-inducing compounds to conserve cardiomyocyte function in experimental atrial fibrillation

Denise M. S. van Marion[1#], Xu Hu[1#], Deli Zhang[1], Femke Hoogstra-Berends[2], Jean-Paul G. Seerden[3], Lizette Loen[3], André Heeres[3,4], Herman Steen[5], Robbert H. Henning[2] and Bianca J. J. M. Brundel[1]

[1]Department of Physiology, Amsterdam Cardiovascular Sciences, VU University Medical Center, Amsterdam, The Netherlands

[2]Department of Clinical Pharmacy and Pharmacology, University Medical Center Groningen, Groningen, The Netherlands

[3]Syncom BV, Groningen, The Netherlands

[4]Hanze University of Applied Sciences, Groningen, The Netherlands

[5]Chaperone Pharma BV, Groningen, The Netherlands

[#]Equal contribution

Drug Design, Development and Therapy. 2019 Jan; 13:345-36

Keywords: atrial fibrillation, heat shock protein, *Drosophila*, proteostasis, geranylgeranylacetone

Abstract

Background The heat shock protein (HSP) inducer, geranylgeranylacetone (GGA), was previously found to protect against atrial fibrillation (AF) remodeling in experimental model systems. Clinical application of GGA in AF is limited, due to low systemic concentrations owing to the hydrophobic character of GGA.

Objectives To identify novel HSP-inducing compounds, with improved physicochemical properties, that prevent contractile dysfunction in experimental model systems for AF.

Methods 81 GGA-derivatives were synthesized and explored for their HSP-inducing properties by assessment of HSP expression in HL-1 cardiomyocytes pre-treated with or without a mild heat shock (HS), followed by incubation with 10 µM GGA or GGA-derivative. Subsequently, the most potent HSP-inducers were tested for preservation of calcium transients (CaT) amplitudes or heart wall contraction in pre-treated tachypaced HL-1 cardiomyocytes (with or without HSPB1 siRNA) and *Drosophilas*, respectively. Finally, CaT recovery in tachypaced HL-1 cardiomyocytes post-treated with GGA or protective GGA-derivatives was determined.

Results Thirty GGA-derivatives significantly induced HSPA1A expression after HS, and seven showed exceeding HSPA1A expression compared to GGA. GGA and nine GGA-derivatives protected significantly from tachypacing (TP) -induced CaT loss, which was abrogated by HSPB1 suppression. GGA and four potent GGA-derivatives protected against heart wall dysfunction after TP compared to non-paced control *Drosophila*s. Of these compounds, GGA and three GGA-derivatives induced a significant restoration from CaT loss after tachypacing of HL-1 cardiomyocytes.

Conclusion We identified novel GGA-derivatives with improved physicochemical properties compared to GGA. GGA-derivatives, particularly GGA*-59, boost HSP expression resulting in prevention and restoration from TP-induced remodeling, substantiating their role as novel therapeutics in clinical AF.

Introduction

Atrial fibrillation (AF) is the most common human cardiac arrhythmia with a prevalence of 2.7-6.1 million and 6.5-12.3 million in the USA and EU, respectively in 2010. This prevalence is expected to rise significantly due to the aging population [1]. AF is a persistent disease, characterized by progressive electrical, structural and contractile remodeling of cardiomyocytes, also referred to as electropathology [2, 3]. Current AF therapies are symptomatic and aim for rate control but do not prevent expansion of the arrhythmogenic substrate [4, 5]. As a consequence, most patients eventually develop longstanding persistent AF, which leads to a substantial increase in cardiac morbidity and mortality and warranty of life-long anticoagulant therapy. Despite extensive investigation of the molecular substrate of cardiac remodeling in AF, no effective therapy is available to date.

Research by us and others provide evidence that derailment of proteostasis is a key factor underlying electropathology and AF progression [6-10]. Proteostasis, the homeostasis of protein production, function and breakdown, is important for proper cell function. Accordingly, derailment of proteostasis is associated with AF but also with many age-related protein-misfolding diseases, including Alzheimer's, Parkinson's and Huntington's disease [11]. Derailment of proteostasis contributes importantly to cardiomyocyte remodeling and predisposes to AF in experimental models and in AF patients [6, 7, 9]. The most important chaperones to maintain a balanced proteostasis are the heat shock proteins (HSPs). During stress, the heat shock response (HSR) is stimulated by activation of heat shock transcription factors (HSF), of which HSF1 is the major regulator of HSP transcription in eukaryotes [12]. HSPs consist of five HSP families, i.e. HSPA (HSP70), HSPB (small HSPs), HSPC (HSP90), HSPD (HSP60), and DnaJB (HSP40), each with several family members, (specific) co-factors in various cellular localizations, with distinct and overlapping functions [13, 14]. The family of HSPBs is probably the most important in maintaining proteostasis in cardiomyocytes [15]. Cardiomyocytes express high levels of HSPBs which localize with contractile and microtubule proteins, thereby stabilizing the cardiomyocyte structure, and conserving the contractile and electrophysiological function of the atrial

cardiomyocytes [16-20]. Although HSPB1 levels are induced in atrial tissue samples of patient with paroxysmal AF, HSPB1 levels get exhausted in patients with (longstanding) persistent AF. In addition, in these patients, HSPB1 levels in atrial tissue correlate inversely with the amount of structural remodeling, suggesting that the HSR becomes exhausted in time resulting in derailment of proteostasis, structural remodeling and AF progression [10, 16]. In line, boosting of the endogenous HSR with drugs may constitute an emerging therapeutic strategy for clinical AF. Securing HSP levels at an adequate level may limit the expansion of the AF substrate for the induction of AF and the ensuing progression of paroxysmal to persistent AF [8]. A well-known HSP-inducing compound is geranylgeranylacetone (GGA). GGA is a nontoxic acyclic isoprenoid compound with a retinoid skeleton that is originally used as an anti-ulcer drug in Asian countries [21, 22]. GGA induces HSPs in various tissues, including gastric mucosa, intestine, liver, myocardium, retina, and central nervous system [23, 24]. The protective effect of GGA-induced HSP expression on tachycardia-induced cardiomyocyte remodeling has been observed in atrial cardiomyocytes, and a *Drosophila* model for AF, suggesting that the induction of HSPs by GGA might have potential value for clinical AF [7, 16, 25, 26]. Furthermore, GGA treatment protected from cardiomyocyte remodeling and tachypacing (TP)-induced AF promotion in a dog model for (acute) atrial ischemia and in a heart failure model in rabbits [7, 27, 28]. Notwithstanding the protective effects, the poor physicochemical properties of GGA, including its lipophilic nature (LogP value 6.54) and limited solubility, pose a serious disadvantage to its drugability. The gut mucosal distribution pattern owing to GGA's hydrophobic character hinders its systemic bioavailability [29, 30] and consequently a relative high daily oral dosage of 120 mg/kg was required to treat dogs [7]. To overcome these disadvantages, various GGA-derivatives with improved physicochemical properties were synthesized and tested for their ability to induce a HSR in HL-1 cardiomyocytes and confer protection against TP-induced contractile dysfunction in HL-1 cardiomyocytes and *Drosophila*. Furthermore, favorable GGA-derivatives were studied on their improvement of recovery from contractile dysfunction in tachypaced HL-1 cardiomyocytes.

Material and Methods

Synthesis of GGA-derivatives

The synthesis of the most potent GGA-derivatives is described in the Supplementary materials.

HL-1 mouse atrial cardiomyocytes culture, TP and CaT measurements

HL-1 atrial cardiomyocytes, derived from adult mouse atria, were obtained from dr. William Claycomb (Louisiana State University, New Orleans, USA, institutional approved MTA with laboratory of Brundel) [31] and maintained as described previously [9]. HL-1 cardiomyocytes, seeded on coverslips, were subjected to TP as described before [7, 16] and CaT were measured. In short, the coverslips with HL-1 cardiomyocytes were placed in 4-well rectangular dishes (Nuclon, The Netherlands) and placed into C-Dish100™-Culture Dishes (IonOptix Corporation, MA). Cardiomyocytes were subjected to TP by electrical field stimulation (4,5 Hz with 20-ms pulses) for 8 h via the CPace100™-Culture Pacer (IonOptix Corporation, The Netherlands), since 8 h of TP previously induced significant CaT loss [32].

To measure CaT, HL-1 cardiomyocytes were incubated for 30 min with the Ca^{2+}-sensitive Fluo-4-AM dye (2 μM) (Invitrogen, The Netherlands), followed by 3 washing steps with Dulbecco's Modified Eagle Medium (DMEM, Gibco). CaT were live recorded in Fluo-4-AM loaded cardiomyocytes in full Claycomb medium (at 1 Hz of stimulation in a temperature (37°C) controlled system) by exciting them at 488 nm. Light emitted at 500-550 nm was visually recorded with a 40x objective, using a Solamere-Nipkow-Confocal-Live-Cell-Imaging system (based on a Leica DM IRE2 Inverted microscope). Absolute fluorescent signals were recorded and analyzed with ImageJ software (National Institutes of Health, USA). To compare the fluorescent signals between experiments, the fluorescent signal at any given time (F) was divided by the fluorescent signal at rest (F0) (Fcal = F/F0) [33]. Mean values from each experimental condition were based on measurements of at least 10 cardiomyocytes per condition.

GGA and GGA-derivative treatment and HS

HL-1 cardiomyocytes, seeded into 6 wells plates, were treated with 10 µM GGA or GGA-derivative or control (dimethylsulfoxide, DMSO) for 6 h with or without HS pre-treatment. In case of HS treatment, HL-1 cardiomyocytes were first subjected to a mild HS (44°C) for 10 min, to pre-activate a HS response, followed by 10 min recovery at 37°C before control (DMSO), GGA or GGA-derivative treatment [34]. HL-1 cardiomyocytes were harvested after 6 h for protein or RNA isolation. In case of CaT measurements, HL-1 cardiomyocytes were treated with 10 µM GGA or GGA-derivative or control (DMSO) for 6 h before TP (pre-treatment) or immediately after TP (post-treatment) for 24 h.

To check the HSF1 activation and the effect of a GGA-derivative on HSF1 activation, HL-1 cardiomyocytes were subjected to a mild HS (44°C), recovered for 10 min and treated with DMSO or GGA*-59. Proteins were isolated after 10 min, 30 min, 1 h, 2 h and 6 h recovery periods.

***Drosophila* TP and drug treatment**

Wild-type W1118 *Drosophila* strain was obtained from Genetic Services Inc. (Massachusetts, USA). Flies were maintained on standard Bloomington medium, supplemented with dried yeast powder, at 25°C. After fertilization, adult flies were removed and 200 µL GGA or GGA-derivative (final concentration 100 µM) diluted in demineralized water or control solution (demineralized water with equal amount of DMSO as compounds) was added to the food of the larvae. Larvae consumed the compound/DMSO-containing food for 2-3 days after which prepupae were collected and placed on 1% agarose gel in PBS. Per condition, at least five prepupae were subjected to TP (5 Hz for 20 min) by the use of a C-Pace100 culture pacer (IonOptix Corp). Before and after TP, the hearts of the prepupae were visualized through a microscope at 10x magnification, movies of the beating heart were made (3x 10 sec) before and after TP with a camera and heart wall contractions were calculated in Hz as previously described in [6, 26, 34].

Protein isolation and Western blot analysis

HL-1 cardiomyocytes were lysed on ice with 125 µL SDS sample loading buffer (10% SDS, 50% glycerol, 0.33 M Tris–HCl pH 6.8, 10% β-mercaptoethanol, 0.05% bromophenol blue) and passed through a syringe. After centrifugation, supernatant was collected and boiled for 6 min. Equal amounts of protein (20 µg) were separated on SDS-PAGE 4-20% PreciseTM Protein gels (Thermo Fisher Scientific, USA) and transferred onto nitrocellulose membranes (GE Healthcare, The Netherlands). Membranes were blocked in 5% skim milk for 1 h at room temperature. Overnight incubation at 4°C with primary antibody (mouse-anti-HSPA1A, Enzo-Lifesciences, USA and Rabbit-anti-HSF1, Cell Signaling Technology, USA) was followed by secondary horseradisch peroxidase-conjugated antibody (goat-anti-mouse or goat-anti-rabbit, Dako Cytomation, Denmark) incubation for 1 h at room temperature. Western blot signals of at least two independent experiments with HL-1 cardiomyocytes were detected by Super Signal (Thermo Scientific, The Netherlands) and quantified by densitometry. The amount of protein was expressed relative to GAPDH.

RNA isolation and PCR analysis

Total RNA was extracted from HL-1 cardiomyocytes by using the NucleoSpin® II RNA isolation kit (Macherey-Nagel, Germany). cDNA was synthesized according to standard methods, using random hexamers, reverse transcriptase (RT), RT buffer, dNTP's and RNAsin (Promega, USA). 1 µg cDNA per reaction in triplicate was used as a template for real-time reverse-transcriptase PCR (qRT-PCR) which was supplemented with SYBRGreen Rox mix (5 µL per sample, Thermo Fisher Scientific, USA), primers (0,3 µL of 10 µM) (see Table 1) and water. mRNA levels were expressed in relative units based on the standard curve (serial dilutions of a pooled cDNA mix) and normalized against GAPDH.

Table 1. Primers for real-time reverse-transcriptase PCR

Protein	Forward	Reverse
HSPA1A (HSP70)	5′ – CATCAAGAAGGTGGTGAAGC – 3′	5′ – ACCACCCTGTTGCTGTAG – 3′
HSPB1 (HSP25)	5′ – TGTATTTCCGGGTGAAGCAC – 3′	5′ – CAGTGAAGACCAAGGAAGGC-3′
HSPCA (HSP90)	5′ – ATTGGTTGGTCTTGGGTCTG – 3′	5′ – GCCAGTTGCTTCAGTGTCCT – 3′
DNAJB1 (HSP40)	5′ – TCCGTGGAATGTGTAGCTGA – 3′	5′ – GATTTTCGACCGCTATGGAG – 3′
HSPA5 (GRP75)	5′ – ATCTTTGGTTGCTTGTCGCT – 3′	5′ – ATGAAGGAGACTGCTGAGGC – 3′
GAPDH	5′ – GCAAGGAGAAGCAGCAGAGT – 3′	5′ – TTTGTGTTTGGACTCTCCCC – 3′

Short interfering RNA HSPB1 knock-down

HL-1 cardiomyocytes were cultured on coverslips coated with 0.02% gelatin in Claycomb medium. After 24 h (80-90% confluency) HL-1 cardiomyocytes were co-transfected with the reporter construct CD8 and siRNA-HSPB1 construct in a ratio of 1:3 (siRNA-HSPB1: from 5′ to 3′; forward, GATCCCC GACCAAGGATGGCGTGGTG TTCAAGAGA CACCACGCCATCCTTGGTC TTTTTA; reverse, AGCTTAAAAA GACCAAGGATGGCGTGGTG TCTCTTGAA CACCACGCCATCCTTGGTC GGG) or as a control for transfection with mock siRNA (forward, GATCCCC GCTGCAAAATCCGATGAGA TTCAAGAGA TCTCATCGGATTTTGCAGC TTTTTA; reverse, AGCTTAAAAA GCTGCAAAATCCGATGAGA TCTCTTGAA TCTCATCGGATTTTGCAGC GGG) in 1 mL Optimem with 3 µL of lipofectamine2000 per well. 24 h after transfection GGA or GGA-derivatives were added to the medium (final concentration 10 µM), incubated for 8 h and followed by TP or non-pacing for 8 h. After loading the cardiomyocytes with the Fluo-4-AM dye, cardiomyocytes were incubated with anti-CD8 coated beads (11147D, Thermo Fisher). CaT measurements were performed only on viable, CD8 positive cardiomyocytes. For each condition, we measured at least 10 cardiomyocytes.

Statistics

Data are presented as mean ± SD or SEM. All experiments were performed at least in duplicate series. Individual group mean differences were evaluated with the Student's *t*-test. Multiple-group comparisons were obtained by ANOVA with Bonferroni corrected post hoc *t*-tests. A 2-tailed $P<0.05$ was considered statistically significant. GraphPad version 7 was used for all statistical evaluations.

Results

Synthesis of a GGA-derivate library

In order to overcome the high lipophilicity of GGA, we first truncated the east side of the molecule to geranylacetone (GA) (Figure 1). Based on this parent structure, a library of 81 compounds was prepared, considering the Lipinski rule of five [35] (Table 2). Not only the east and west side of the molecule were varied but also several bio-isosters of the central keto-moiety of GA were designed and prepared. The keto-moiety of GGA and truncated derivatives was replaced by isosteric groups, such as oxime, amide, sulfonamide, ester, hydroxyl, pyrazolone, pyrazole and oxazole moieties. For the east and west side variations, different alkyl chains were chosen, sometimes containing additional functional groups (hydrogen bond donors and acceptors), including aromatics. The strategy used to prepare GGA-derivatives is depicted in Figure 1; see Supplementary materials for a detailed description of synthesis. Following this strategy, almost all GGA-derivatives reveal an improved LogP value, compared to the mother compound GGA (LogP 6.54), having a molecular weight below 500 (Table 2).

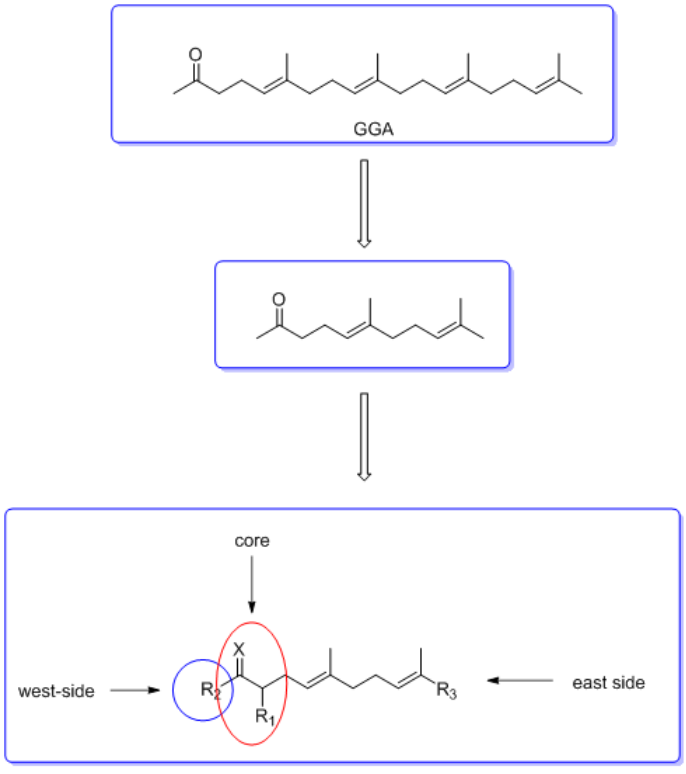

Figure 1. Design and synthesis of a compound library based upon GGA/GA

The east side of the molecule to geranylacetone (GA) was truncated, variations were made at the east and west side of the molecule and several bio-isosters of the central keto moiety were prepared.

Table 2. Overview of physicochemical, HSP-inducing properties, and cardio-protective effects of GGA-derivatives in HL-1 cardio

Compound		Physicochemical properties			
		Structural formula	Molecular formula	Molecular weight	LogP
GGA		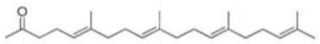	$C_{23}H_{38}O$	330,56	6,54
FA		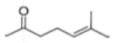	$C_{18}H_{30}O$	262,43	5,02
GA		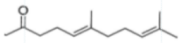	$C_{13}H_{22}O$	194,32	3,49
GGA analog	GGA*-01	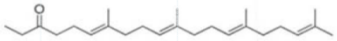	$C_{24}H_{40}O$	344,57	7,2
	GGA*-02	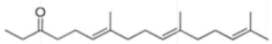	$C_{19}H_{32}O$	276,46	5,67
	GGA*-03	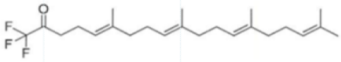	$C_{23}H_{35}F_3O$	384,52	7,03
	GGA*-04	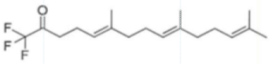	$C_{18}H_{27}F_3O$	316,4	5,5
	GGA*-05	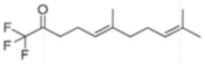	$C_{13}H_{19}F_3O$	248,28	3,97
	GGA*-06	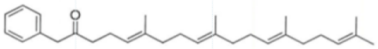	$C_{29}H_{42}O$	406,64	7,72
	GGA*-07	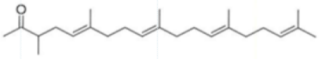	$C_{24}H_{40}O$	344,57	7,11
Geranyl oxims	GGA*-08	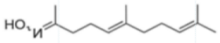	$C_{13}H_{23}NO$	209,33	3,88
and keto-iso-oxalzoles	GGA*-09	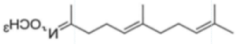	$C_{14}H_{25}NO$	223,35	4,14
	GGA*-10	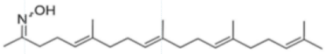	$C_{23}H_{39}NO$	345,56	6,93
	GGA*-11	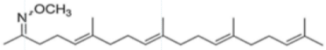	$C_{24}H_{41}NO$	359,59	7,19
geranyl keto-esters	GGA*-12	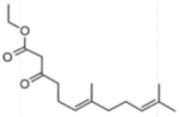	$C_{16}H_{26}O_3$	266,38	3,16
	GGA*-13	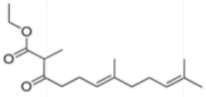	$C_{17}H_{28}O_3$	280,4	3,72
	GGA*-14	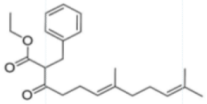	$C_{23}H_{32}O_3$	356,5	5,33
	GGA*-15	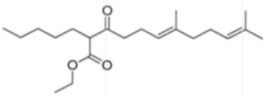	$C_{21}H_{36}O_3$	336,51	5,39
	GGA*-16	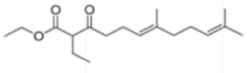	$C_{18}H_{30}O_3$	294,43	4,14
	GGA*-17	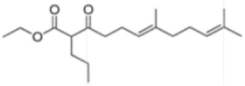	$C_{19}H_{32}O_3$	308,46	4,56

myocyte model and *Drosophila*

		HL-1 mouse atrial cardiomyocytes						*Drosophila melanogaster*	
H-bond acceptor	**H-bond donor**	**HSPA1A boosting (protein)**		**CaT (pre-treatment)**		**CaT (post-treatment)**		**Contractile function**	
		Fold induction ± SD	***P-value***	**Protection (yes/no)**	***P-value***	**Protection (yes/no)**	***P-value***	**Protection (yes/no)**	***P-value***
√		37 ± 15	<0.01	Yes	<0.0001	Yes	<0.0001	Yes	<0.0001
√		0.6 ± 0.4							
√		39 ± 17	<0.01						
√		0.52 ± 0.32							
√		1 ± 1.07							
√		0.25 ± 0.08							
√		52 ± 19	<0.01						
√		78 ± 11	<0.01						
√		43 ± 11	<0.01						
√		32 ± 9	<0.01						
√	√	0.57 ± 0.54							
√		0.57 ± 0.7							
√	√	0.5 ± 0.16							
√		0.48 ± 0.07							
√		0.44 ± 0.08							
√		0.52 ± 0.4							
√		160 ± 21	<0.0001	No					
√		0.33 ± 0.08							
√		0.37 ± 0.2						No	
√		0.41 ± 0.2							

Compound		Physicochemical properties			
		Structural formula	Molecular formula	Molecular weight	LogP
	GGA*-18	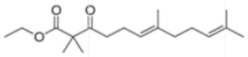	$C_{18}H_{30}O_3$	294,43	4,43
	GGA*-19	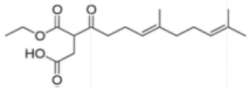	$C_{18}H_{28}O_5$	324,41	2,74
	GGA*-20	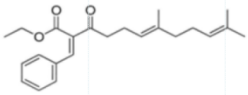	$C_{23}H_{30}O_3$	354,48	5,09
	GGA*-21	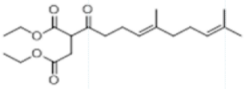	$C_{20}H_{32}O_5$	352,45	3,34
	GGA*-22	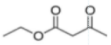	$C_6H_{10}O_3$	130,14	-0,13
	GGA*-23	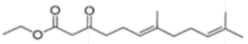	$C_{16}H_{30}O_3$	270,41	4,1
	GGA*-24	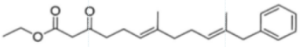	$C_{22}H_{30}O_3$	342,47	4,76
	GGA*-25	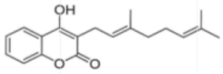	$C_{19}H_{22}O_3$	298,38	4,15
	GGA*-26	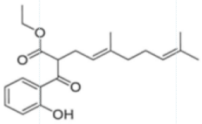	$C_{21}H_{28}O_4$	344,44	4,48
	GGA*-27	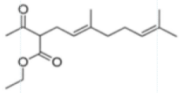	$C_{16}H_{26}O_3$	266,38	3,07
pyrazolones	GGA*-28	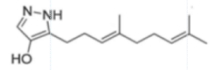	$C_{14}H_{22}N_2O$	234,34	3,92
	GGA*-29	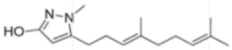	$C_{15}H_{24}N_2O$	248,36	4,15
	GGA*-30	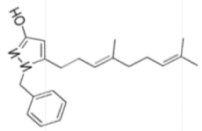	$C_{21}H_{28}N_2O$	324,46	5,89
diketones	GGA*-31	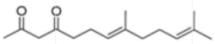	$C_{15}H_{24}O_2$	236,35	1,09
Geranyl ketones I	GGA*-32	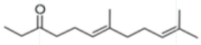	$C_{14}H_{24}O$	208,34	4,14
	GGA*-33	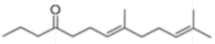	$C_{15}H_{26}O$	222,37	4,56
	GGA*-34	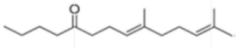	$C_{16}H_{28}O$	236,39	4,98
	GGA*-35	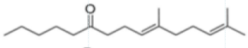	$C_{17}H_{30}O$	250,42	5,4
	GGA*-36	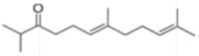	$C_{15}H_{26}O$	222,37	4,71
Geranyl ketones II	GGA*-37	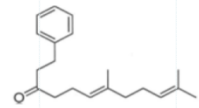	$C_{20}H_{28}O$	284,44	5,75
	GGA*-38	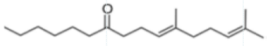	$C_{18}H_{32}O$	264,45	5,81
	GGA*-39	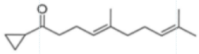	$C_{15}H_{24}O_2$	220,35	4,21
	GGA*-40	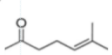	$C_8H_{14}O$	126,2	1,96

		HL-1 mouse atrial cardiomyocytes						*Drosophila melanogaster*	
H-bond acceptor	H-bond donor	HSPA1A boosting (protein)		CaT (pre-treatment)		CaT (post-treatment)		Contractile function	
		Fold induction ± SD	*P-value*	Protection (yes/no)	*P-value*	Protection (yes/no)	*P-value*	Protection (yes/no)	*P-value*
√		101 ± 14	<0.001	Yes	<0.0001			No	
√		0.4 ± 0.2							
√		15 ± 7	<0.05						
√		13 ± 5	<0.05						
√		0.3 ± 0.2							
√		17 ± 4							
√		0.5 ± 0.3							
√	√	0.4 ± 0.2							
√	√	31 ± 10	<0.01	Yes	<0,01				
√		0.3 ± 0.1							
√	√	78 ± 8	<0.01	Yes	<0.0001	No		No	
√	√	0.4 ± 0.4							
√	√	0.5 ± 0.2							
√		155 ± 20	<0.0001	Yes	<0.0001	Yes	<0,05	Yes	<0,05
√		32 ± 16	<0.01	Yes	<0.05				
√		1 ± 1							
√		15 ± 12	<0.05						
√		14 ± 10	<0.05						
√		0.5 ± 0.08							
√		0.3 ± 0.3							
√		0.5 ± 0.56							
√		0.4 ± 0.5							
√		0.65 ± 0.3							

Compound		Physicochemical properties			
		Structural formula	Molecular formula	Molecular weight	LogP
	GGA*-41		$C_{19}H_{26}O$	270,41	5,1
	GGA*-42	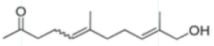	$C_{13}H_{22}O_2$	210,31	2,43
	GGA*-43	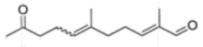	$C_{13}H_{20}O_2$	208,3	2,29
	GGA*-44	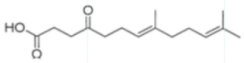	$C_{15}H_{24}O_3$	252,35	5,75
pyrazoles/isoxazoles	GGA*-45	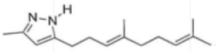	$C_{15}H_{24}N_2$	232,36	4,3
	GGA*-46	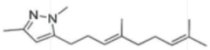	$C_{16}H_{26}N_2$	246,39	4,53
	GGA*-47	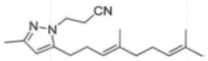	$C_{18}H_{27}N_3$	285,43	4,57
	GGA*-48	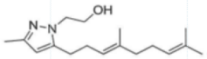	$C_{17}H_{28}N_2O$	276,42	4,01
	GGA*-49	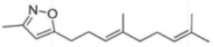	$C_{15}H_{23}NO$	233,35	4,37
	GGA*-50	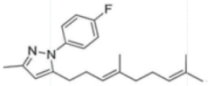	$C_{21}H_{27}FN_2$	326,45	6,35
	GGA*-51	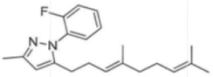	$C_{21}H_{27}FN_2$	326,45	6,35
	GGA*-52	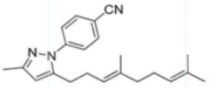	$C_{22}H_{27}N_3$	333,47	6,23
isosters	GGA*-53	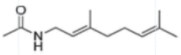	$C_{12}H_{21}NO$	195,3	2,04
	GGA*-54	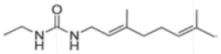	$C_{13}H_{24}N_2O$	222,34	2,29
	GGA*-55	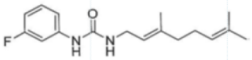	$C_{17}H_{23}FN_2O$	290,38	3,77
	GGA*-56	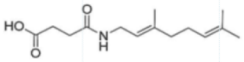	$C_{14}H_{23}NO_3$	253,34	1,71
	GGA*-57	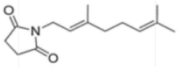	$C_{14}H_{21}NO_2$	235,32	1,96
	GGA*-58	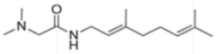	$C_{14}H_{26}N_2O$	238,37	1,86
	GGA*-59	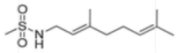	$C_{11}H_{21}NO_2S$	231,35	1,59
	GGA*-60	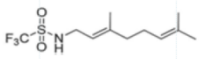	$C_{11}H_{18}F_3NO_2S$	285,33	3,77
	GGA*-61	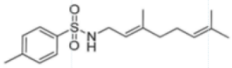	$C_{17}H_{25}NO_2S$	307,45	4,26
	GGA*-62	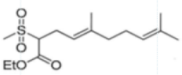	$C_{15}H_{26}O_4S$	302,43	2,14
	GGA*-63	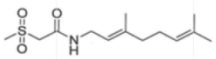	$C_{13}H_{23}NO_3S$	273,39	0,69
	GGA*-64	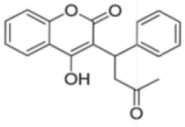	$C_{19}H_{16}O_4$	308,33	2,97
	GGA*-65	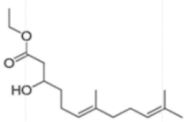	$C_{16}H_{28}O_3$	268,39	3,33

		HL-1 mouse atrial cardiomyocytes						*Drosophila melanogaster*	
H-bond acceptor	**H-bond donor**	**HSPA1A boosting (protein)**		**CaT (pre-treatment)**		**CaT (post-treatment)**		**Contractile function**	
		Fold induction ± SD	***P-value***	**Protection (yes/no)**	***P-value***	**Protection (yes/no)**	***P-value***	**Protection (yes/no)**	***P-value***
√		0.62 ± 0.2							
√	√	0.42 ± 0.008							
√		0.9 ± 0.8							
√		13 ± 3	<0.05						
√	√	15 ± 5	<0.05						
√		14 ± 8	<0.05						
√		0.4 ± 0.5							
√	√	0.5 ± 0.3							
√		0.4 ± 0.2							
√		0.3 ± 0.2							
√		0.6 ± 0.4							
√		0.4 ± 0.2							
√	√	0.6 ± 0.3							
√	√	0.4 ± 0.3							
√	√	0.3 ± 0.2							
√	√	33 ± 8	<0.01	No					
√	√	90 ± 12	<0.001	Yes	<0.0001			No	
√	√	95 ± 14	<0.001	Yes	<0.0001	No		Yes	<0,01
√	√	157 ± 19	<0.0001	Yes	<0.0001	Yes	<0.0001	Yes	<0.0001
√	√	162 ± 21	<0.0001	Yes	<0.0001	Yes	<0.0001	Yes	<0,01
√	√	15 ± 5	<0.05						
√		0.3 ± 0.2							
√	√	0.4 ± 0.3							
√	√	0.4 ± 0.4							
√	√	0.6 ± 0.3							

Compound		Physicochemical properties			
		Structural formula	Molecular formula	Molecular weight	LogP
	GGA*-66	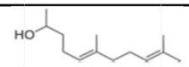	$C_{13}H_{24}O$	196,33	3,5
	GGA*-67	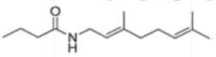	$C_{14}H_{25}NO$	223,45	3,11
	GGA*-68	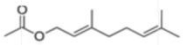	$C_{12}H_{20}O_2$	196,29	2,72
	GGA*-69	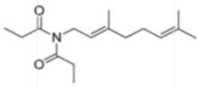	$C_{16}H_{27}NO_2$	265,39	3,3
	GGA*-70	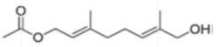	$C_{12}H_{20}O_3$	212,29	1,66
	GGA*-71	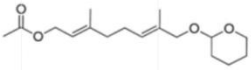	$C_{17}H_{28}O_4$	296,4	2,86
not in a group	GGA*-72	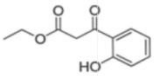	$C_{11}H_{12}O_4$	208,21	1,28
	GGA*-73	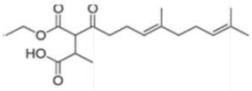	$C_{19}H_{30}O_5$	338,44	3,3
	GGA*-74	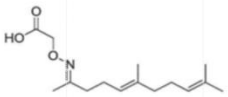	$C_{15}H_{25}NO_3$	267,36	3,14
	GGA*-75	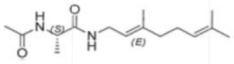	$C_{15}H_{26}N_2O_2$	266,38	1,38
	GGA*-76	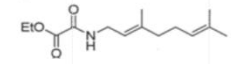	$C_{14}H_{23}NO_3$	253,34	2,42
	GGA*-77	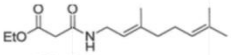	$C_{15}H_{25}NO_3$	267,36	2,36
	GGA*-78	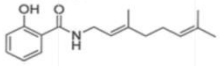	$C_{17}H_{23}NO_2$	273,37	3,55
	GGA*-79		$C_4H_5O_2$	88,11	0,29
	GGA*-80	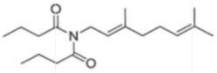	$C_{18}H_{31}NO_2$	293,44	4,13
	GGA*-81	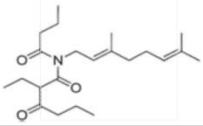	$C_{22}H_{37}NO_3$	363,53	4,69

Note: The table provides the information of all subsequent experiments. The first columns gives information on the first experiments were all compounds were used, the later experiments are shown in the later columns, where not all compounds are used. When information is given for a certain column, the compound is used, and when a cell is blank, the compound is not tested used for that experiment.

		HL-1 mouse atrial cardiomyocytes						*Drosophila melanogaster*	
H-bond acceptor	**H-bond donor**	**HSPA1A boosting (protein)**		**CaT (pre-treatment)**		**CaT (post-treatment)**		**Contractile function**	
		Fold induction ± SD	***P-value***	**Protection (yes/no)**	***P-value***	**Protection (yes/no)**	***P-value***	**Protection (yes/no)**	***P-value***
√	√	0.5 ± 0.1							
√	√	13 ± 3	<0.05						
√		0.3 ± 0.1							
√		0.3 ± 0.4							
√	√	15 ± 4	<0.05						
√		17 ± 6	<0.05						
√	√	33 ± 8	<0.01	No					
√		0.6 ± 0.2							
√	√	0.4 ± 0.2							
√	√	45 ± 6	<0.001	No					
√	√	0.2 ± 0.1							
√	√	0.5 ± 0.1	<0.05						
√	√	0.6 ± 0.4							
√		22 ± 5	<0.05						
√		0.7 ± 0.5							
√		0.3 ± 0.1							

GGA and GGA-derivatives boost HSF1-related HSP expression in HL-1 cardiomyocytes

HSP-inducing properties of the 81 synthesized GGA-derivatives and GGA were explored in HL-1 cardiomyocytes (Table 2). Since HSPA1A is expressed at low basal levels (compared to abundant basal levels of HSPB1) in non-stressed control HL-1 cardiomyocytes and becomes strongly upregulated upon a HS, HSPA1A was used as a read-out. When non-stressed control HL-1 cardiomyocytes were treated for 6 h with 10 µM GGA or GGA-derivatives, a minor induction of HSPA1A expression was observed by Western blot analysis (Figure S1). Post-treatment with 10 µM GGA or 81 GGA-derivatives after a mild, non-lethal HS (10 min 44°C, 10 min recovery 37°C) revealed 30 derivatives that significantly elevated HSPA1A expression compared to control. The HSPA1A boosting effect of GGA-derivatives was comparable to or significantly larger compared to GGA (Figure 2A,B).

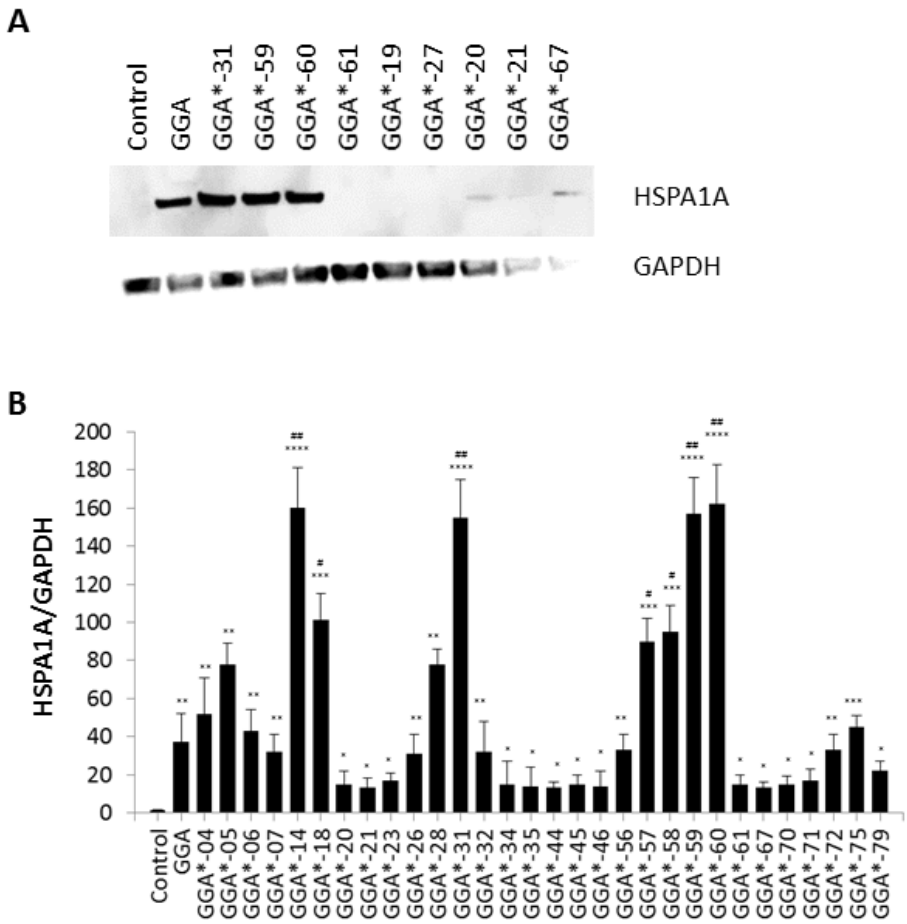

Figure 2. GGA and GGA-derivatives induce HSPA1A expression in HL-1 cardiomyocytes pre-treated with GGA and GGA-derivatives upon a mild HS

(**A**) Representative example of a Western blot for HSPA1A and GAPDH of HL-1 cardiomyocytes pre-treated with DMSO (Control), 10 µM GGA and 10 µM GGA*-19, -20, -21, -27, -31, -59, -60, -61 and -67 upon a mild HS.

(**B**) Quantified Western blot results for HSPA1A relative to GAPDH for GGA and GGA-derivatives. Mean ± SEM, **P*<0.05, ***P*<0.01, ****P*<0.001 and *****P*<0.0001 compared to control cardiomyocytes and $^{\#}P$<0.05 and $^{\#\#}P$<0.01 compared to GGA.

The HSPA1A boosting effect could not be linked to a specific group of molecular structures of GGA-derivatives (Figure S2). Next to boosting of HSPA1A expression levels, GGA-derivatives elevated mRNA expression of HSF1-mediated HSPs, including HSPA1A, HSPB1, DNAJB1 and HSPCA, while mRNA levels of the non-HSF1-related HSPA5 were unaffected (Figure S3). Together, the data suggest that GGA and 30 GGA-derivatives boost HSP expression in HL-1 cardiomyocytes most likely via HSF1 regulation. At identical concentrations, seven GGA-derivatives boosted protein abundance of HSPA1A to levels exceeding those of GGA (Figure 2B).

Table 3. Overview of cardio-protective effects of the most potent HSPA1A inducers in HL-1 cardiomyocyte model and *Drosophila*

GGA-derivative	HL-1 mouse cardiomyocytes				*Drosophila melanogaster*	
	CaT (pre-treatment)		CaT (post-treatment)		Contractile function	
	Protection vs control (yes/no)	*P*-value	Protection vs 24 h recovery (yes/no)	*P*-value	Protection vs control (yes/no)	*P*-value
GGA	Yes	<0.0001	Yes	<0.0001	Yes	<0.0001
GGA*-14	No	-	-	-	-	-
GGA*-18	Yes	<0.0001	-	-	No	-
GGA*-26	Yes	<0.01	-	-	-	-
GGA*-28	Yes	<0.0001	No	-	No	-
GGA*-31	Yes	<0.0001	Yes	<0,05	Yes	<0,05
GGA*-32	Yes	<0.05	-	-	-	-
GGA*-56	No	-	-	-	-	-
GGA*-57	Yes	<0.0001	-	-	No	-
GGA*-58	Yes	<0.0001	No	-	Yes	<0,01
GGA*-59	Yes	<0.0001	Yes	<0.0001	Yes	<0.0001
GGA*-60	Yes	<0.0001	Yes	<0.0001	Yes	<0.01
GGA*-72	No	-	-	-	-	-

'-' is not applicable

GGA and GGA-derivatives protect against CaT loss in tachypaced HL-1 cardiomyocytes

To examine whether GGA-derivatives, like GGA, protect against contractile dysfunction, HL-1 cardiomyocytes were pre-treated with twelve GGA-derivatives with strong HSPA1A-boosting properties (Table 3) for 8 h, followed by 8 h TP (4.5 Hz) or normal pacing (1 Hz). Previous studies revealed that GGA induces HSPA1A expression up to 24 h upon treatment [7, 16]. Contractile function was determined by measuring CaT. TP induced significant CaT loss compared to normal pacing, which was prevented by GGA and GGA*-18, -26, -28, -31, -32, -57, -58, -59 and -60 (Figure 3).

Suppression of HSPB1 abrogated the protective effect of the GGA-derivative in HL-1 cardiomyocytes

Since previous studies implicate HSPB1 as a crucial HSP in the protective effect of GGA against TP-induced CaT loss [7], we tested whether the protective effect of GGA-derivatives acts via HSPB1. Hereto, HL-1 cardiomyocytes were transfected with siRNA-HSPB1 constructs or control, followed by GGA or GGA-derivative treatment for 8 h, and TP or non-pacing for 8 h. siRNA treatment successfully suppressed HSPB1 24 h after transfection (Figure 4A). siRNA-mediated suppression of HSPB1 levels completely abrogated the protective effect of GGA or GGA-derivatives (Figure 4B,C), indicating that their protective effect is dependent on HSPB1.

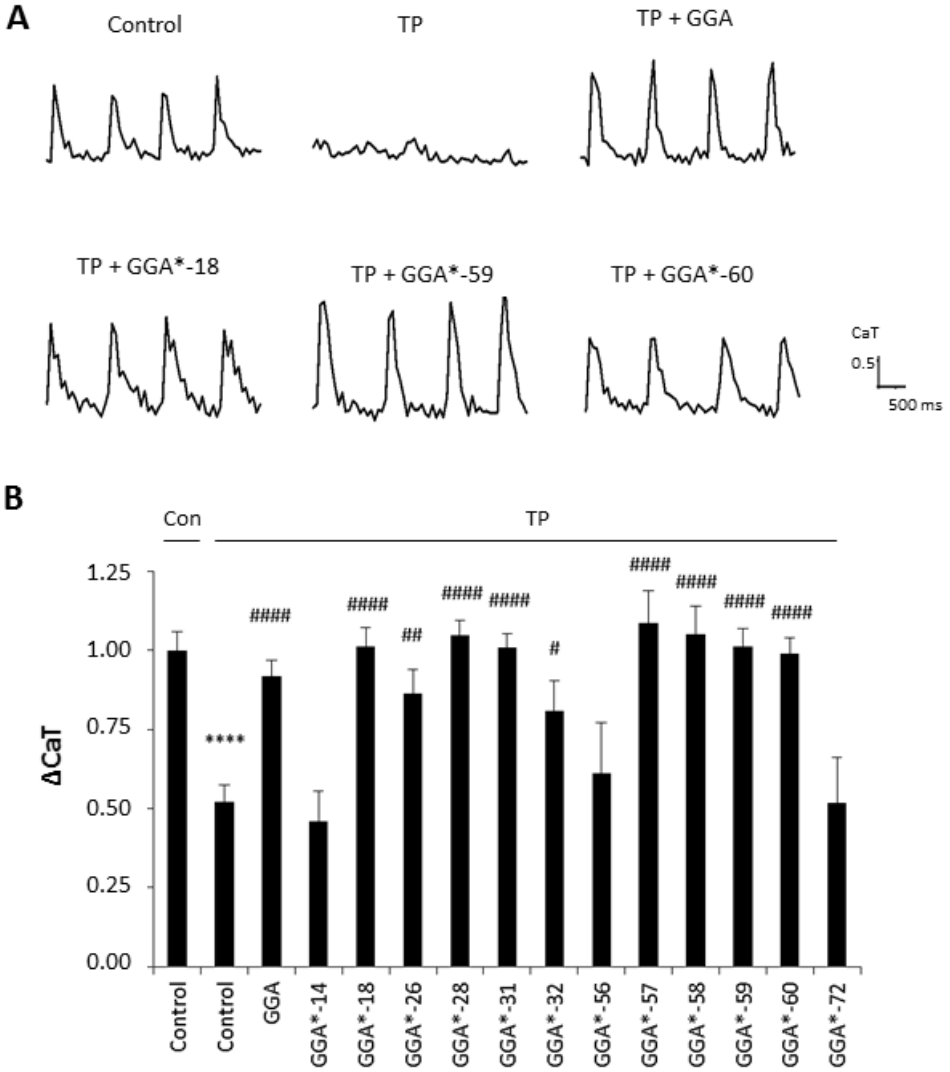

Figure 3. GGA and GGA-derivatives protect against CaT loss in HL-1 cardiomyocytes

Compared to normal-paced controls, TP induces a loss in CaT amplitude which is protected by pre-treatment with GGA and GGA-derivatives. (**A**) Illustrations of CaT tracers of control HL-1 cardiomyocytes (paced at 1 Hz) and of HL-1 cardiomyocytes after 8 h of tachypacing (4.5 Hz) pre-treated with DMSO (TP), 10 µM GGA, or 10 µM GGA*-18, -59, or -60. (**B**) Quantified CaT amplitudes of HL-1 cardiomyocytes treated with DMSO (Control), 10 µM GGA or 10 µM GGA-derivatives. Nine GGA-derivatives, namely GGA*-18, -26, -28, -31, -32, -57, -58, -59 and -60, show significant protection against CaT loss. ****P<0.0001 compared to normal-paced control, $^{\#}P$<0.05, $^{\#\#}P$<0.01 and $^{\#\#\#\#}P$<0.0001 compared to tachypaced control. Notes: The first control is a normal-paced control, treated with DMSO, as indicated by the line above the column with 'Con' above it. The second control is a tachypaced control, treated with DMSO, indicated with the line above the column of tachypaced cells with 'TP' above it.

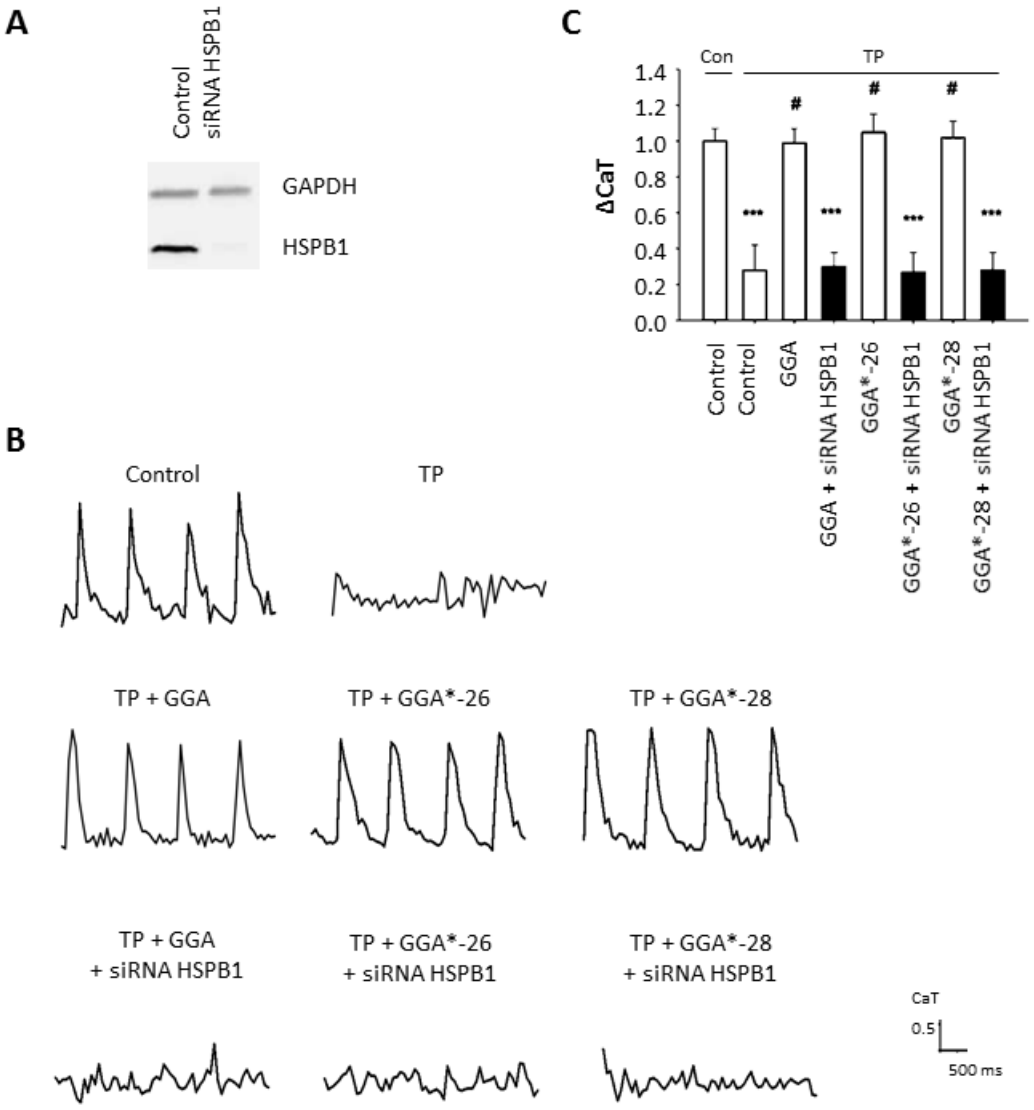

Figure 4. siRNA against HSPB1 abrogated the protective effect of the GGA-derivatives in HL-1 cardiomyocytes

(**A**) Successful suppression of HSPB1 expression in HL-1 cardiomyocytes. (**B**) CaT tracers of control HL-1 cardiomyocytes (paced at 1 Hz) and of HL-1 cardiomyocytes after 8 h of TP (4.5 Hz) pre-treated with DMSO (Control), 10 µM GGA or 10 µM GGA*-26 or 10 µM GGA*-28 show, that HSPB1 knock down abrogate the protective effects of the compounds**.** (**C**) Quantified CaT amplitude of HL-1 cardiomyocytes pre-treated with DMSO (Control), 10 µM GGA or 10 µM GGA*-26 or 10 µM GGA*-28 with/without siRNA against HSPB1. ***P<0.001 compared to normal-paced control cardiomyocytes and $^{\#}P$<0.05 compared to tachypaced control cardiomyocytes. Note: the first control is a normal-paced, DMSO treated control, indicated by the line above the column with 'Con'. The second control is a tachypaced, DMSO treated control, indicated by the line above the column with 'TP'.

GGA and GGA-derivatives protect against contractile dysfunction in *Drosophila*

Next, we assessed whether protective GGA-derivatives, identified in HL-1 cardiomyocytes, also protected *Drosophila* from TP-induced contractile dysfunction. Hereto, the seven most protective GGA-derivatives (GGA*-18, -28, -31, -57, -58, -59 and -60, Table 3) and, as a negative control, one non-HSPA1A boosting GGA-derivative (GGA*-16), were examined. All compounds were without effect on basal heart function (Figure S4). TP for 20 min at 5 Hz induced a significant dysfunction of heart wall contractility (Figure 5 and Videos S1 and S2), which was prevented by GGA and GGA*-31, -58, -59 and -60 (Figure 5 and Videos S3 and S4). Expectedly, GGA*-16 was without effect, because of its lack of protection in HL-1 cardiomyocytes (Figure 5). These findings indicate that four GGA-derivatives protect against TP-induced contractile dysfunction in the *Drosophila* model for AF.

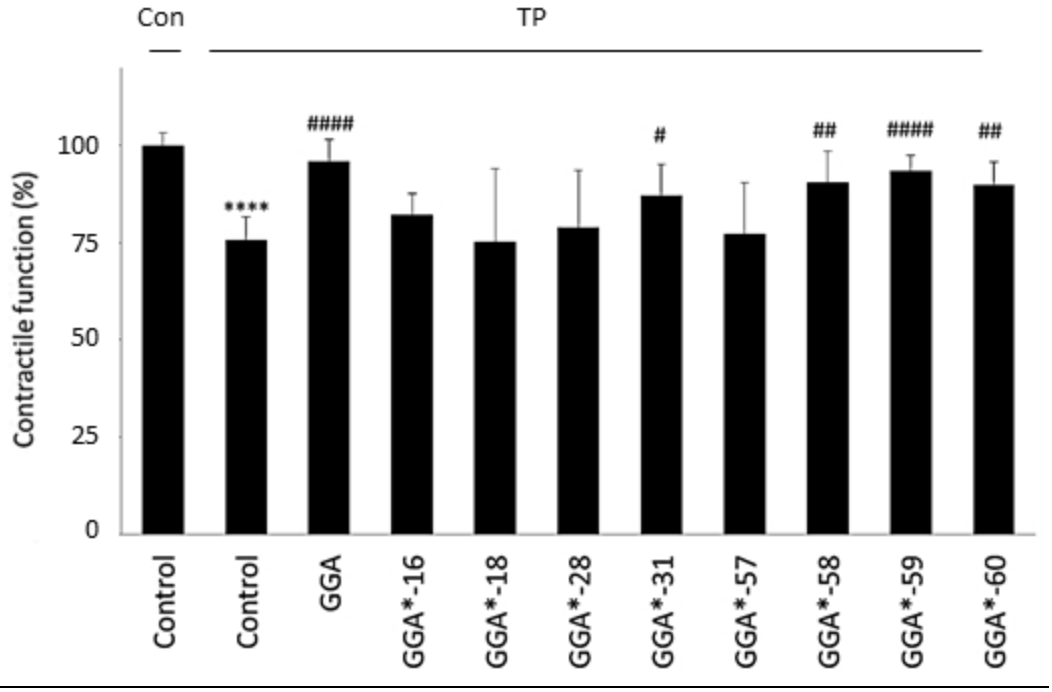

Figure 5. GGA and GGA-derivatives protect against contractile dysfunction in *Drosophila*

TP (5 Hz) induces significant heart wall contractile dysfunction in *Drosophila*. *Drosophila* prepupae pre-treated with 100 µM GGA, 100 µM GGA*-31, -58, -59 or -60 were protected against TP-induced contractile dysfunction, while GGA*-16, -18, -28 or -57 were not protective. Mean ± SEM, ****P<0.0001 compared to non-paced Control prepupae, $^{\#}P$<0.05, $^{\#\#}P$<0.01 and $^{\#\#\#\#}P$<0.0001 compared to tachypaced control prepupae. Note: the first control is a non-paced control, treated with DMSO. The second control is a tachypaced control, treated with DMSO.

GGA-derivatives restore contractile function after TP

Since most patients with AF reveal cardiomyocyte remodeling at the moment of diagnosis, compounds that restore contractile function are of high clinical relevancy. Therefore, GGA-derivatives were tested for their ability to restore CaT loss in the tachypaced HL-1 cardiomyocyte model. Hereto, HL-1 cardiomyocytes were tachypaced at 4.5 Hz for 8 h, followed 24 h recovery and treatment with GGA or GGA-derivatives (GGA*-28, -31, -58, -59 and -60, Table 3). TP resulted in a significant CaT loss, which even further decreased after 24 h recovery (Figure 6A,B). However, tachypaced HL-1 cardiomyocytes post-treated with 10 µM GGA*-31, -59 or -60 or GGA significantly restored CaT, compared to untreated HL-1 cardiomyocytes. Restoration of CaT by GGA and GGA*-59 was significantly larger than GGA*-31 and -60 at 10 µM, while GGA*-28 and -58 did not restore contractile function (Figure 6A,B). These findings indicate that GGA and GGA*-59 restore cardiomyocyte function after TP, whilst GGA*-28, -31, -58 and -60 do not or to a lesser extent.

HSF1 activation by GGA-derivative

Finally, to address the mode of action of the top functional GGA-derivative, we assessed the effect of GGA*-59 (10 µM) on the main effector of GGA effects, i.e. HSF1 phosphorylation status [36], by assessing HSF1 mobility on SDS-PAGE. HS induces activation of HSF1, as indicated by decreased mobility because of HSF1 hyperphosphorylation [37], lasting for up to 1 h (Figure 7A,B). Treatment with GGA*-59 enhances the ratio of hyperphosphorylated HSF1/HSF1 (Figure 7A,B), thus further enhancing HSF1 activation. In accord, treatment with GGA*-59 enhances subsequent HSPA1A protein expression (Figure 7C,D). These data signifies that GGA*-59 boosts HSPs via HSF1 activation.

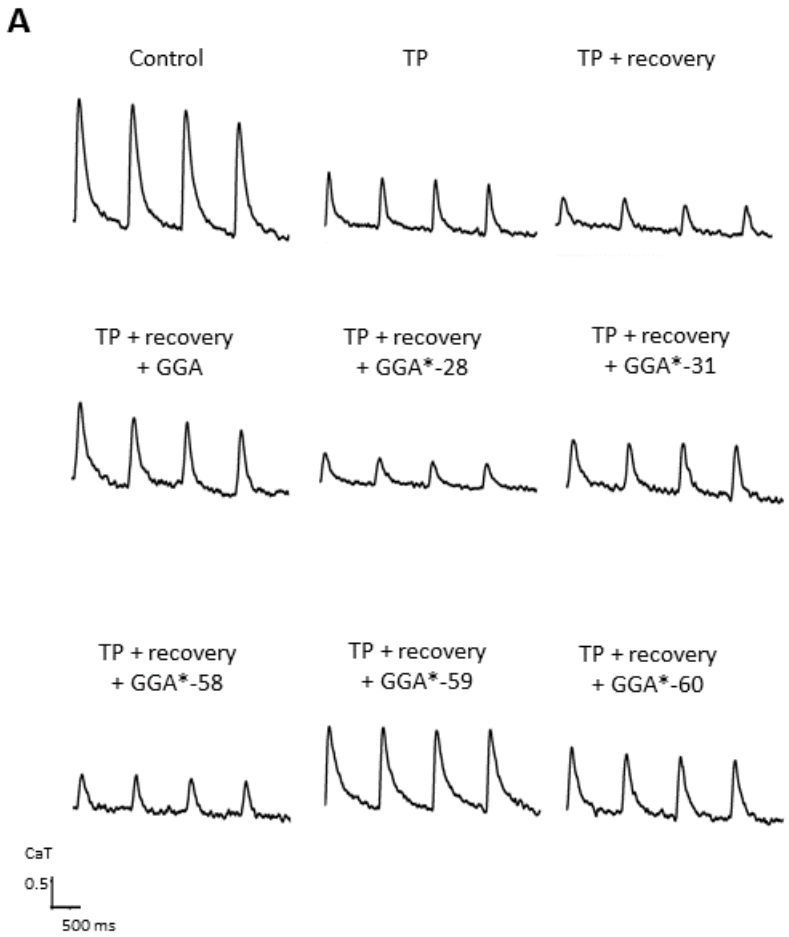

Figure 6. GGA and GGA*-31, -59 and -60 accelerate restoration of CaT loss in HL-1 atrial cardiomyocytes after 24 h post-treatment, compared to the non-treated cardiomyocytes

(**A**) CaT of Control, TP, TP with 24 h recovery and TP with 24 h recovery in combination with post-treatment with 10 µM GGA or GGA-derivatives.

(**B**) Quantified data revealing that GGA and GGA*-31, -59 and -60 accelerate restoration of CaT loss in HL-1 atrial cardiomyocytes after 24 h post-treatment. ****P<0.0001 compared to control cardiomyocytes, $^{\#}P$<0.05; $^{\#\#\#\#}P$<0.0001 compared to tachypaced cardiomyocytes that recovered for 24 h and $^{\dagger}P$<0.05 and $^{\dagger\dagger\dagger\dagger}P$<0.0001 compared to GGA*-59. Note: The first control is a normal-paced control, treated with DMSO, indicated by the line above the column with 'Con'. The second control is a tachypaced control, treated with DMSO, indicated by the line above the columns with 'TP'.

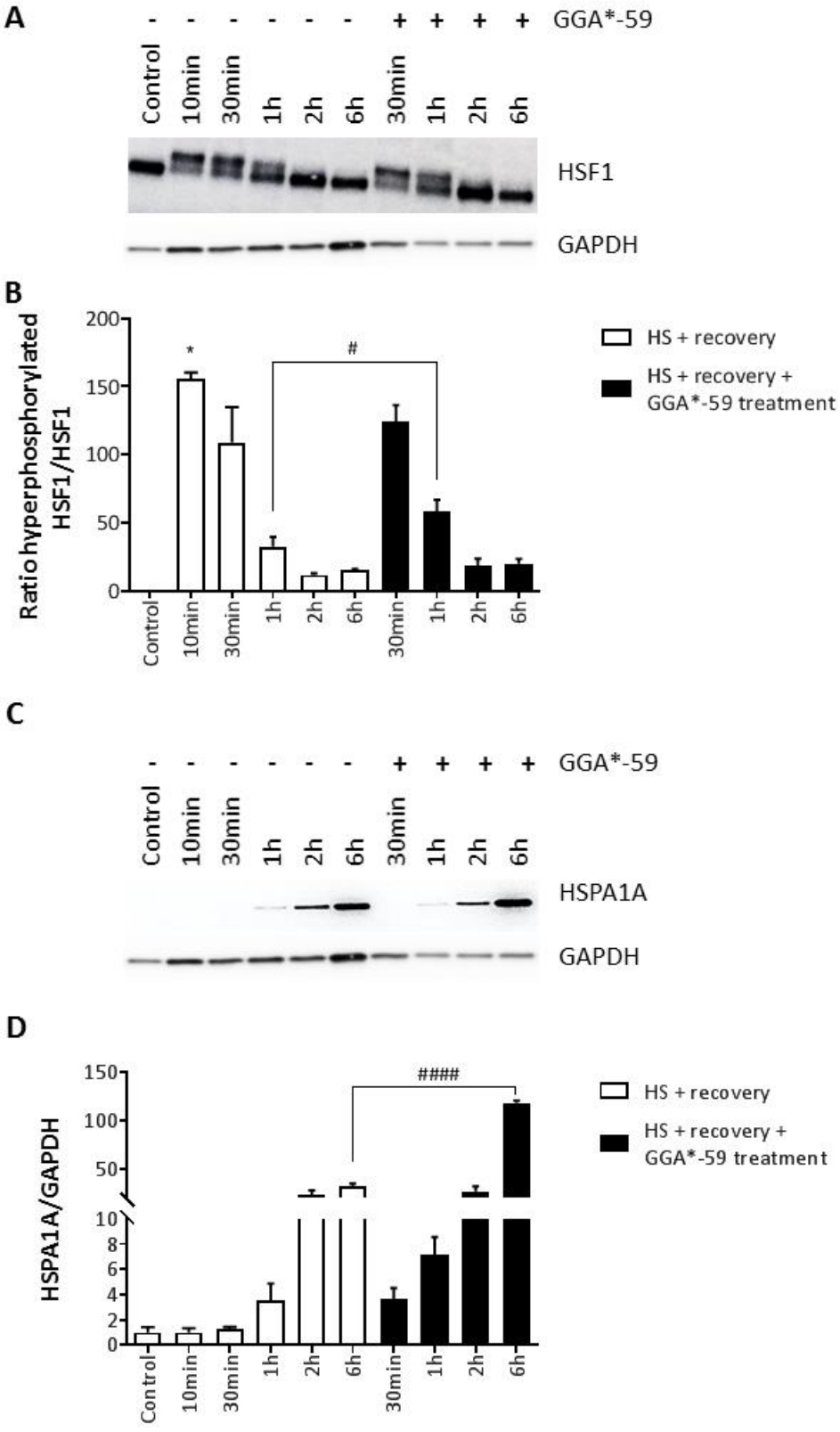

Figure 7. GGA*-59 enhances HSF1 hyper-phosphorylation and subsequent HSPA1A boosting in HL-1 cardiomyocytes

(**A**) GGA*-59 enhances hyperphosphorylation of HSF1, shown by decreased mobility of HSF1 in the gel.

B) GGA*-59 enhances the ratio of hyper-phosphorylated HSF1/ HSF1 (quantified higher band/lower band).

(**C**) Representative Western blot showing HSPA1A expression levels for the conditions as indicated.

(**D**) GGA*-59 treatment enhances HSPA1A protein expression levels after 6 h treatment, compared to non-treated heat shocked control cardio-myocytes.

*P<0.05 compared to Control, $^{\#}P$<0.05 and $^{\#\#\#\#}P$<0.0001 compared to non-treated cardiomyocytes at 1 h and 6 h, respectively.

Discussion

Previous studies identified the HSP-booster GGA to protect against contractile dysfunction and remodeling in experimental models for AF [7, 16, 25, 26, 38]. However, its lipophilic character hampers systemic bioavailability in patients [30]. Since HSPs may limit AF progression and possibly reverse remodeling in clinical AF, we here report on the structural properties of novel derivatives of GGA. 81 GGA-derivatives were synthesized by shortening the lipophilic backbone of GGA and modifying the east, west and central part of the molecule. Seven out of 30 GGA-derivatives that significantly induced HSPA1A expression after a mild HS were superior to GGA, at the given dose, in terms of higher HSPA1A protein expression. Nine out of the twelve most potent HSPA1A boosters (GGA*-18, -26, -28, -31, -32, -57, -58, -59 and -60) protected against TP-induced loss of CaT in HL-1 cardiomyocytes and four GGA-derivatives (GGA*-31, -58, -59 and -60) also protected against contractile dysfunction in *Drosophila* prepupae, which consumed GGA-derivative supplemented food during their larval stage as a pre-treatment. Protective effects of GGA-derivatives seem dependent of HSPB1, because siRNA against HSPB1 abrogates the protection from TP-induced CaT loss, as previously found for GGA [7]. Intriguingly, post-treatment, i.e. with GGA and GGA-derivatives (GGA*-31, -59 and -60 of which GGA*-59 was superior compared to GGA*-31 and -60) directly after TP for the duration of 24 h, restored TP-induced CaT loss in HL-1 cardiomyocytes. Not all GGA-derivatives which revealed protective effects against CaT loss in HL-1 cardiomyocytes were also protective upon pre-treatment in tachypaced *Drosophila* or could restore cardiomyocyte function upon 24 h post-treatment (Table 3). This may be due to reduced stability of the derivative. Future studies should elucidate the pharmacokinetics of potent GGA-derivatives. Nevertheless, we identified one GGA-derivative, GGA*-59, with improved physicochemical properties, that boosts HSPs, and both protects from TP-induced contractile dysfunction, and restores this after TP. Consequently, our analysis indicates GGA*-59 as a GGA-derivative with substantial potential for clinical applications.

Improved physicochemical properties of GGA-derivatives

The clinical use of GGA to treat AF is hampered by its lipophilicity and therefore high dosages have to be used [7, 39]. Here we report a library of GGA-derivatives, created considering the Lipinski rule of five [35], to achieve more druggable analogues of GGA while maintaining *in vitro*/*in vivo* activity. The improved physicochemical properties of the GGA-derivatives, essentially having LogP values between 0 and 5 and molecular weight below 500, increase their solubility and are expected to improve passage of lipid bilayers, most likely resulting in increased uptake in the intestine and improved distribution to the body and cells [35], thereby improving clinical applicability.

The derivatives that boosted HSP expression and protected against and induced recovery (only GGA*-31, -59 and-60) from TP-induced contractile dysfunction were GGA*-57, -58, -59 and -60 (isosters from GGA), GGA* -14, -18 and -26 (“geranyl keto esters”) and GGA*-28 (“a geranyl ketone”). Despite the fact that the most favorable compounds are divided into groups based on the isosteric (central part) and east- and west-side modifications, we were unable to attribute this to specific structural features of the compounds. Further research/synthesis is needed to expand the hits to series of lead compounds with clinical potential.

Preserving proteostasis: possible mode of action of GGA-derivatives

Given the similarity of the actions of the efficacious GGA-derivatives to GGA effects, the most likely mode of action of our derivatives comprises their preservation of proteostasis by activation of HSF1 and subsequent boosting of HSPs expression. The observed increase in gene expression levels of various HSF1-regulated genes by GGA-derivatives, including HSPA1A, HSPB1, DNAJB1, HSPCA, and absence of increase in the HSF1-independent HSPA5, are similar to GGA. In addition, similar to GGA [36], GGA*-59 prolonged HSF1 activation, as shown by its increased hyperphosphorylation. Collectively, these data indicate that GGA-derivatives boost HSP expression by prolonging HSF1

activation, resulting in its extension of binding to the heat shock element (HSE) in the promotor regions of *hsp* genes, thus prolonging *hsp* gene transcription and HSP protein expression. At least, 30 GGA-derivatives significantly induced HSPA1A protein expression of which seven demonstrated improved HSP-boosting properties compared to GGA.

The precise nature of the molecular pathway by which GGA and GGA-derivatives prolong hyperphosphorylation of HSF1 is still subject of speculation. It is known that geranyl-groups act as post-translational modifiers of proteins, and thereby regulate protein function [40]. Natural occurring prenylation with C15 (farnesyl) or C20 (geranylgeranyl) isoprenoids, derived from mevalonic acid, mediates translocation of RhoA to the plasma membrane and activation of the downstream pathway [41-43]. In addition, active RhoA was found to abrogate the HSF1 transcriptional activity by suppressing HSF1 binding to the HSE of *hsp* genes [37]. Therefore, one of the possible mechanisms constitute the competition of GGA and GGA-derivatives with endogenous geranyl-groups, which could lead to inhibition of RhoA activation, resulting in enhanced binding of HSF1 to the HSE region [44, 45]. However, this should be further investigated by genetic ablation, competition and enhanced binding experiments.

How HSPs protect the cardiomyocytes

Irrespective of the precise molecular pathways affected by GGA and GGA-derivatives, their protective action seems critically dependent on boosting HSPB1, because the protective effect was abrogated by siRNA against HSPB1. In previous studies, HSPB1 overexpression protected from TP-induced contractile dysfunction and structural remodeling in HL-1 and *Drosophila* models for AF [7, 26]. HSPB1 stabilizes sarcomeric proteins, including alpha-actinin and actin, prevents their disruption and enhances recovery after disruption [20, 46]. Furthermore, HSPB1 (co)-localizes with myosin in HL-1 cardiomyocytes and at myofilaments in human atrial myocytes and thereby potentially conserve myofibrils [16]. Therefore, HSPB1 may shield the contractile proteins from AF-induced cleavage by

cysteine proteases, such as calpain [26, 47, 48]. Given that GGA-derivatives enhance HSP expression and protect from TP-induced contractile dysfunction, which is abrogated after suppression of HSPB1, we appoint HSPB1 to be one of the most important players in the cardio-protective effect of GGA-derivatives.

Therapeutic application of HSP-inducing compounds

In this study, HSP-inducing compounds were shown to prevent and reverse contractile dysfunction in experimental models for AF, which is promising for treating clinical AF, since patients diagnosed with AF already suffer from AF-related electropathology. Besides, comparable to GGA, the GGA-derivatives only boosted the HSR in cardiomyocytes pre-treated with a mild, sub-lethal HS and not under non-stressed conditions, indicating that augmentation of the HSR by GGA and its derivatives is confined to stressed cells. In clinical perspective, this might indicate that side effects due to enhancing HSR are limited, if existent at all. Accordingly, it would be of interest to test suitable GGA-derivatives for future applications in the clinic. This would initially require testing of selected GGA-derivatives in a larger *in vivo* model for AF, such as the atrial pacemaker stimulated dog model for AF. Although the experimental models used in the current study were suitable to extract potent HSP boosters from the 81 synthesized GGA-derivatives, they do not fully reflect the complexity of electropathology in AF, making extrapolation to clinical AF beyond reach. Furthermore, pharmacokinetics need to be further explored in *in vivo* models to investigate bioavailability of the derivatives. Yet, GGA itself could already be further explored in clinical AF despite its less favorable physicochemical therapeutic profile, since the compound is already marketed in various Asian countries and considered a safe drug. As a proof of concept, a first study may explore whether GGA induces HSP expression in atrial tissue of AF patients and whether induced HSP expression correlates to reduced AF burden. Further research is necessary to test whether GGA or GGA-derivatives can prevent progression of clinical AF and reverse existing electropathology in clinical AF.

Conclusion

We identified multiple GGA-derivatives, especially GGA*-59, with an improved physicochemical profile and full preservation of HSP-boosting capacities, including both cardio-protective properties and acceleration of recovery from contractile dysfunction in an experimental model of AF. As such, this study substantiates our previous findings that HSP induction has high potential as a novel approach to prevent progression of AF and reverse remodeling.

Abbreviations AF: atrial fibrillation; Con: control; CaT: calcium transient; cDNA: copy deoxyribonucleic acid; DMEM: Dulbecco's Modified Eagle Medium; DMSO: dimethylsulfoxide; dNTP's: deoxy nucleoside triphosphates; FA: farnesylacetone; FBS: fetal bovine serum; GA: geranylacetone; GAPDH: glycerylaldehyde 3-phosphate dehydrogenase; GGA: geranylgeranylacetone; HS(R): heat shock (response); HSF1: heat shock factor 1; HSP: heat shock protein; MTA: material transfer agreement; PBS: phosphate buffered saline; qRT-PCR: quantitative real-time reverse-transcriptase poly chain reaction; RT: reverse transcriptase; SD: standard deviation; SDS-(PAGE): sodium dodecyl sulfate (polyacrylamide gel electrophoresis); siRNA: short interfering ribonucleic acid; TP: tachypacing

Acknowledgments

This work was supported by the Dutch Heart Foundation (2013T144 and 2013T096) and the Netherlands Cardiovascular Research Initiative and Dutch Heart Foundation (CVON2014-40 DOSIS and CVON-STW2016-14728 AFFIP), the European Community, European Fund for Regional Development (Operationeel Programma Noord-Nederland 2007-2012, OP-EFRO), the Life Sciences & Health-Impulse grant (40-43100-98-008), and the Province of Groningen, Innovative Action-program Groningen (IAG3)

Author contributions

All authors contributed toward data analysis, drafting and critically revising the paper, gave final approval of the version to be published, and agreed to be accountable for all aspects of the work.

Disclosure

Jean-Paul G. Seerden, Lizette Loen, and André Heeres are employees of Syncom BV. Herman Steen is the founder and CEO of Chaperone Pharma BV, a pharmaceutical company engaged in clinical development of HSP boosting drugs. The authors report no other conflicts of interest in this work.

References

1. Mozaffarian D, et al. Heart disease and stroke statistics--2015 update: a report from the American Heart Association. Circulation 2015;131(4):e29-322.
2. De Groot NM, et al. Electropathological substrate of longstanding persistent atrial fibrillation in patients with structural heart disease: epicardial breakthrough. Circulation 2010;122(17):1674-82.
3. Allessie MA, et al. Electropathological substrate of long-standing persistent atrial fibrillation in patients with structural heart disease: longitudinal dissociation. Circ Arrhythm Electrophysiol 2010;3(6):606-15.
4. Dobrev D, et al. Novel molecular targets for atrial fibrillation therapy. Nat Rev Drug Discov 2012;11(4):275-91.
5. Camm AJ, et al. 2012 focused update of the ESC Guidelines for the management of atrial fibrillation: an update of the 2010 ESC Guidelines for the management of atrial fibrillation. Developed with the special contribution of the European Heart Rhythm Association. Eur Heart J 2012;33(21):2719-47.
6. Zhang D, et al. Activation of histone deacetylase-6 induces contractile dysfunction through derailment of alpha-tubulin proteostasis in experimental and human atrial fibrillation. Circulation 2014;129(3):346-58.
7. Brundel BJ, et al. Induction of heat shock response protects the heart against atrial fibrillation. Circ Res 2006;99(12):1394-402.
8. Lanters EA, et al. The future of atrial fibrillation therapy: intervention on heat shock proteins influencing electropathology is the next in line. Neth Heart J 2015;23(6):327-33.
9. Wiersma M, et al. Endoplasmic Reticulum Stress Is Associated With Autophagy and Cardiomyocyte Remodeling in Experimental and Human Atrial Fibrillation. J Am Heart Assoc 2017;6(10):e006458.
10. Henning RH and Brundel B. Proteostasis in cardiac health and disease. Nat Rev Cardiol 2017;14(11):637-653.
11. Balch WE, et al. Adapting proteostasis for disease intervention. Science 2008;319(5865):916-9.

12. Baler R, et al. Activation of human heat shock genes is accompanied by oligomerization, modification, and rapid translocation of heat shock transcription factor HSF1. Mol Cell Biol 1993;13(4):2486-96.
13. Haslbeck M, et al. Some like it hot: the structure and function of small heat-shock proteins. Nat Struct Mol Biol 2005;12(10):842-6.
14. Kim HJ, et al. Heat shock responses for understanding diseases of protein denaturation. Mol Cells 2007;23(2):123-31.
15. Golenhofen N, et al. Comparison of the small heat shock proteins alphaB-crystallin, MKBP, HSP25, HSP20, and cvHSP in heart and skeletal muscle. Histochem Cell Biol 2004;122(5):415-25.
16. Brundel BJ, et al. Heat shock protein upregulation protects against pacing-induced myolysis in HL-1 atrial myocytes and in human atrial fibrillation. J Mol Cell Cardiol 2006;41(3):555-62.
17. Kotter S, et al. Human myocytes are protected from titin aggregation-induced stiffening by small heat shock proteins. J Cell Biol 2014;204(2):187-202.
18. Bullard B, et al. Association of the chaperone alphaB-crystallin with titin in heart muscle. J Biol Chem 2004;279(9):7917-24.
19. Ghosh JG, et al. Interactive domains in the molecular chaperone human alphaB crystallin modulate microtubule assembly and disassembly. PLoS One 2007;2(6):e498.
20. Bryantsev AL, et al. Distribution, phosphorylation, and activities of Hsp25 in heat-stressed H9c2 myoblasts: a functional link to cytoprotection. Cell Stress Chaperones 2002;7(2):146-55.
21. Murakami M, et al. Antiulcer effect of geranylgeranylacetone, a new acyclic polyisoprenoid on experimentally induced gastric and duodenal ulcers in rats. Arzneimittelforschung 1981;31(5):799-804.
22. Yanaka A, et al. Geranylgeranylacetone protects the human gastric mucosa from diclofenac-induced injury via induction of heat shock protein 70. Digestion 2007;75(2-3):148-55.
23. Katsuno M, et al. Pharmacological induction of heat-shock proteins alleviates polyglutamine-mediated motor neuron disease. Proc Natl Acad Sci U S A 2005;102(46):16801-6.
24. Hirakawa T, et al. Geranylgeranylacetone induces heat shock proteins in cultured guinea pig gastric mucosal cells and rat gastric mucosa. Gastroenterology 1996;111(2):345-57.
25. Brundel BJ, et al. Heat shock proteins as molecular targets for intervention in atrial fibrillation. Cardiovasc Res 2008;78(3):422-8.
26. Zhang D, et al. Effects of different small HSPB members on contractile dysfunction and structural changes in a Drosophila melanogaster model for Atrial Fibrillation. J Mol Cell Cardiol 2011;51(3):381-9.
27. Sakabe M, et al. Effects of a heat shock protein inducer on the atrial fibrillation substrate caused by acute atrial ischaemia. Cardiovasc Res 2008;78(1):63-70.
28. Chang SL, et al. Heat shock protein inducer modifies arrhythmogenic substrate and inhibits atrial fibrillation in the failing heart. Int J Cardiol 2013;168(4):4019-26.
29. Porter CJ, et al. Lipids and lipid-based formulations: optimizing the oral delivery of lipophilic drugs. Nat Rev Drug Discov 2007;6(3):231-48.
30. Nishizawa YY, et al. Metabolic fate of geranylgeranylacetone. Drug Metabolism and Pharmacokinetics 1986;1(2):171-177.
31. Claycomb WC, et al. HL-1 cells: a cardiac muscle cell line that contracts and retains phenotypic characteristics of the adult cardiomyocyte. Proc Natl Acad Sci U S A 1998;95(6):2979-84.
32. Ke L, et al. HSPB1, HSPB6, HSPB7 and HSPB8 protect against RhoA GTPase-induced remodeling in tachypaced atrial myocytes. PLoS One 2011;6(6):e20395.
33. Paredes RM, et al. Chemical calcium indicators. Methods 2008;46(3):143-51.
34. Den Hoed M, et al. Identification of heart rate-associated loci and their effects on cardiac conduction and rhythm disorders. Nat Genet 2013;45(6):621-31.
35. Lipinski CA, et al. Experimental and computational approaches to estimate solubility and permeability in drug discovery and development settings. Adv Drug Deliv Rev 2001;46(1-3):3-26.

36. Anckar J and Sistonen L. Regulation of HSF1 function in the heat stress response: implications in aging and disease. Annu Rev Biochem 2011;80:1089-115.
37. Meijering RA, et al. RhoA Activation Sensitizes Cells to Proteotoxic Stimuli by Abrogating the HSF1-Dependent Heat Shock Response. PLoS One 2015;10(7):e0133553.
38. Hoogstra-Berends F, et al. Heat shock protein-inducing compounds as therapeutics to restore proteostasis in atrial fibrillation. Trends Cardiovasc Med 2012;22(3):62-8.
39. Luo FC, et al. Geranylgeranylacetone protects mice against morphine-induced hyperlocomotion, rewarding effect, and withdrawal syndrome. Free Radic Biol Med 2012;52(7):1218-27.
40. Shack S, et al. Activation of the cholesterol pathway and Ras maturation in response to stress. Oncogene 1999;18(44):6021-8.
41. Rattan S. 3-Hydroxymethyl coenzyme A reductase inhibition attenuates spontaneous smooth muscle tone via RhoA/ROCK pathway regulated by RhoA prenylation. Am J Physiol Gastrointest Liver Physiol 2010;298(6):G962-9.
42. Yang J, et al. Alteration of RhoA Prenylation Ameliorates Cardiac and Vascular Remodeling in Spontaneously Hypertensive Rats. Cell Physiol Biochem 2016;39(1):229-41.
43. Cook M, et al. Increased RhoA prenylation in the loechrig (loe) mutant leads to progressive neurodegeneration. PLoS One 2012;7(9):e44440.
44. Sysa-Shah P, et al. Geranylgeranylacetone blocks doxorubicin-induced cardiac toxicity and reduces cancer cell growth and invasion through RHO pathway inhibition. Mol Cancer Ther 2014;13(7):1717-28.
45. Hashimoto K, et al. Geranylgeranylacetone inhibits lysophosphatidic acid-induced invasion of human ovarian carcinoma cells in vitro. Cancer 2005;103(7):1529-36.
46. Lavoie JN, et al. Modulation of cellular thermoresistance and actin filament stability accompanies phosphorylation-induced changes in the oligomeric structure of heat shock protein 27. Mol Cell Biol 1995;15(1):505-16.
47. Garrido C, et al. HSP27 inhibits cytochrome c-dependent activation of procaspase-9. FASEB J 1999;13(14):2061-70.
48. Concannon CG, et al. Hsp27 inhibits cytochrome c-mediated caspase activation by sequestering both pro-caspase-3 and cytochrome c. Gene Expr 2001;9(4-5):195-201.

Supplemental Information

Material and Methods

Synthesis of GGA-derivatives

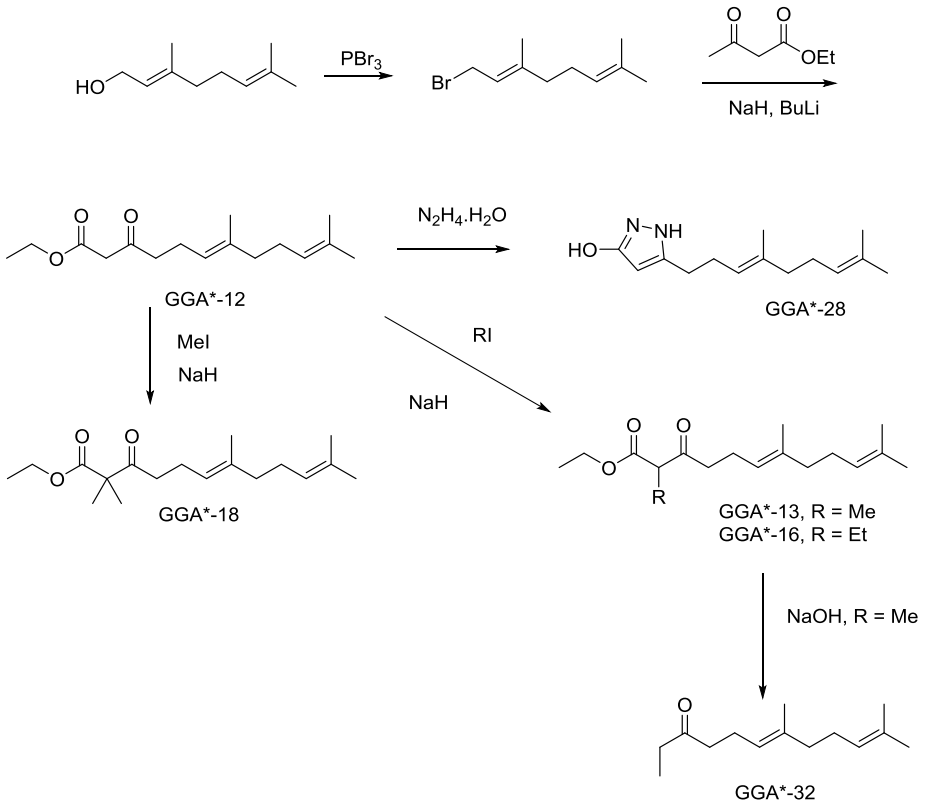

Synthesis of GGA-12, -13, -16, -28 and -32*

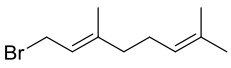

(*E*)-1-bromo-3,7-dimethylocta-2,6-diene. Geraniol (10 g, 11.4 mL, 64.8 mmol, 1.0 eq) was dissolved in DCM (50 mL), under a nitrogen atmosphere. The solution was cooled to -20 °C. A solution of PBr_3 (3.0 mL, 32.4 mmol, 0.5 eq) in DCM (10 mL) was added drop-wise, keeping the temperature < -16 °C. The color changed to green/blue during addition. The reaction mixture was stirred for 3h at ~ -20 °C. Water (50 mL) was added carefully at -40 °C. The water layer was extracted with Et_2O (3 x 50 mL). The combined organic layers were washed with sat. aq. NH_4Cl. sol. (3 x 50 mL), dried over Na_2SO_4 and concentrated *in vacuo* to provide a brown oil (14.5 g, 66.6 mmol, 100%.)

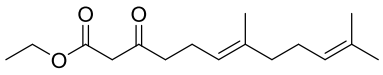

GGA*-12

(E)-Ethyl 7,11-dimethyl-3-oxododeca-6,10-dienoate (GGA*-12). NaH (60% in oil, 2.63 g, 65.8 mmol, 1.0 eq) was suspended in THF (20 mL), under a nitrogen atmosphere. The solution was cooled to 0 °C with an ice/water bath. Ethylacetoacetate (8.3 mL, 65.8 mmol, 1.0 eq) was added drop-wise in 1 h. During addition a thick suspension was formed which later became a yellow solution. Gas formation was visible and an exothermic reaction was observed. The temperature was kept <10 °C. The reaction mixture was stirred for 10 min at 0 °C. n-BuLi (2.5M in hexanes, 26.3 mL, 65.8 mmol, 1.0 eq) was added drop-wise in 10 min. An very exothermic reaction was observed, during addition the flask was cooled with an ice/MeOH bath. A bright yellow suspension was formed which changed into a yellow solution. The temperature was kept at 0 °C for 10 min. Geranylbromide (ABCR, 9.1 mL, 46.1 mmol, 0.7 eq) was added drop-wise and a suspension was formed. The reaction mixture was warmed to RT and stirred for 1 h. The reaction mixture was poured in sat. aq. NH_4Cl sol. (100 mL) and the water layer was extracted with TBME (3 x 100 mL). The combined organic layers were dried over Na_2SO_4 and concentrated *in vacuo* to provide a yellow oil (17.1 g). The crude product was purified by automated column chromatography (eluens, 0 to 100% DCM in heptanes) affording a colorless oil (6.0 g, 22.4 mmol, 49%).

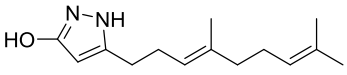

GGA*-28

(E)-5-(4,8-dimethylnona-3,7-dien-1-yl)-1H-pyrazol-3-ol (GGA*-28). GGA*-12 (500 mg, 1.88 mmol, 1.0 eq) was dissolved in EtOH (10 mL), under a nitrogen atmosphere. The solution was cooled to 0°C with an ice/water bath. Hydrazine (64% water, 0.12 mL, 2.44 mmol, 1.3 eq) was added and the solution was warmed to RT overnight. The solvents were removed *in vacuo* and Et_2O (10 mL) was added to the

residue. The solids were isolated by filtration and purified by automated column chromatography (eluens, 50 to 100% EtOAc in heptanes) yielding a white solid (81 mg, 0.35 mmol, 18%).

^{1}H-NMR ($CDCl_3$, in ppm): 1.61 (s, 3H), 1.64 (s, 3H), 1.69 (s, 3H), 2.03 (m, 4H), 2.37 (m, 2H), 2.42 (t, 1H), 2.60 (t, 1H), 5.17 (m, 2H), HPLC-MS: $(M+1)^+$ = 235,2

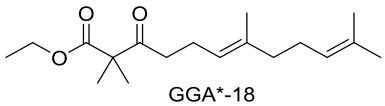

GGA*-18

(E)-ethyl 2,2,7,11-tetrameyhyl-3-oxododeca-6,10-dienoate (GGA*-18). NaH (70 mg, 1.8 mmol, 2.6 eq) was suspended in TFH (6 mL), under a nitrogen atmosphere, and cooled to 0°C with an ice/water bath. A solution of GGA*-12 (180 mg, 0.68 mmol, 1.0 eq) in THF (20 mL) was added and the solution was allowed to warm to RT and subsequently stirred for 30 min at this temperature. A solution of MeI (101 μL, 1.6 mmol, 2.4 eq) in THF (20 mL) was added and the solution was heated to reflux temperature and stirred overnight. The solvents were removed *in vacuo*. Water (30 mL) was added and the water layer was extracted with TBME (3 x 30 mL) and EtOAc (1 x 30 mL). The combined organic layers were dried over Na_2SO_4 and concentrated *in vacuo*. The crude product was purified by automated column chromatography (eluens 0 to 100% DCM in heptanes) affording a colorless oil (20.1 mg, 0.068 mmol, 10%)

^{1}H-NMR ($CDCl_3$, in ppm): 1.21 (t, 3H), 1.38 (s, 6H), 1.59 (s, 3H), 1.60 (s, 3H), 1.63 (s, 3H), 2.00 (m, 4H), 2.24 (m, 2H), 2.44 (m, 2H), 4.18 (q, 2H), 5.03 (m, 2H), HPLC-MS: $(M+1)^+$ = 295,2

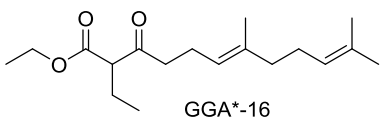

GGA*-16

(E)-Ethyl-2-ethyl-7,11-dimethyl-3-oxododeca-6,10-dienoate (GGA*-16). NaH (60% in oil, 39 mg, 0.98 mmol, 1.3 eq) was suspended in THF (6 mL), under a nitrogen atmosphere, and cooled to 0 °C with an ice/water bath. A solution of GGA*-12 (200 mg, 0.75 mmol, 1.0 eq) in THF (20 mL) was added and the

solution was warmed to RT and stirred for 30 min. A solution of iodoethane (72 μL, 0.90 mmol, 1.2 eq) in THF (20 mL) was added and the mixture was heated at reflux temperature overnight and cooled to RT over the weekend. The solvents were removed *in vacuo*. Water (30 mL) was added and the water layer was extracted with TBME (3 x 30 mL). The combined organic layers were dried over Na_2SO_4 and concentrated *in vacuo*. The crude product was purified by automated column chromatography (eluens 0 to 100% DCM in heptanes) affording a colorless oil (37 mg, 0.13 mmol, 17%).

^{1}H-NMR ($CDCl_3$, in ppm): 0.93 (t, 3H), 1.29 (t, 3H), 1.60 (s, 3H), 1.62 (s, 3H), 1.71 (s, 3H), 2.00 (m, 6H), 2.30 (m, 2H), 2.58 (m, 2H), 3.39 (q, 1H), 4.20 (q, 2H), 5.04 (m, 2H), HPLC-MS: $(M+1)^+$ = 295,2

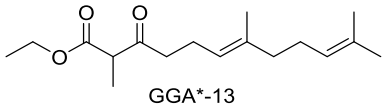

GGA*-13

(E)-Ethyl 2,7,11-trimethyl-3-oxododeca-6,10-dienoate (GGA*-13). NaH (60% in oil, 39 mg, 0.976 mmol, 1.3 eq) was suspended in THF (6 mL), under a nitrogen atmosphere. The solution was cooled to 0 °C with an ice/water bath. A solution of GGA*-12 (200 mg, 0.751 mmol, 1.0 eq) in THF (20 mL) was added and the solution was warmed to room temperature and stirred for 30 min. A solution of MeI (56 μL, 0.90 mmol, 1.2 eq) in THF (20 mL) was added and the reaction mixture was heated at reflux temperature overnight. The THF was removed *in vacuo* and water (25 mL) was added to the residue. The water layer was extracted with TBME (3 x 20 mL). The combined organic layers were dried over Na_2SO_4 and concentrated *in vacuo* to provide a brown oil (367 mg). The crude product was purified twice by automated column chromatography (1. eluens o to 10% EtOAc in heptanes and 2. eluens 0 to 100% DCM in heptanes) affording a colorless oil (24 mg, 0.086 mmol, 9%).

^{1}H-NMR ($CDCl_3$, in ppm): 1.29 (t, 3H), 1,31 (d, 3H), 1.60 (s, 3H), 1.62 (s, 3H), 1.71 (s, 3H), 2.00 (m, 6H), 2.30 (m, 2H), 2.58 (m, 2H), 3.39 (q, 1H), 4.20 (q, 2H), 5.04 (m, 2H), HPLC-MS: $(M+1)^+$ = 281,4

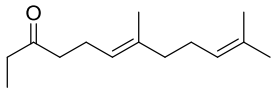

GGA*-32

(E)-7,11-dimethyldodeca-6,10-dien-3-one (GGA*-32). GGA*-13 (24 mg, 0.086 mmol, 1.0 eq) was dissolved in EtOH (5 mL). NaOH (1.2 M, 3.6 mL, 4.3 mmol, 50 eq) was added and the solution was heated at 50 °C for 3h. The solution was acidified with acetic acid and concentrated *in vacuo*. Water (20 mL) was added to the residue and the water layer was extracted with Et_2O (3 x 20 mL). The combined organic layers were dried over Na_2SO_4 and concentrated *in vacuo*. The crude product was purified by automated column chromatography (eluens 0 to 100% DCM in heptanes) affording a colorless oil (18 mg, 0.09 mmol, quant.).

^{1}H-NMR ($CDCl_3$, in ppm): 1.05 (t, 3H), 1.61 (s, 3H), 1,64 (s, 3H), 1.66 (s, 3H), 2.00 (m, 4H), 2.30 (m, 2H), 2.42 (m, 4H), 5.05 (m, 2H), HPLC-MS: $(M+1)^+$ = 209,3

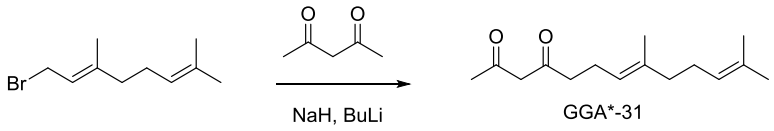

GGA*-31

(E)-8,12-Dimethyltrideca-7,11-diene-2,4-dione (GGA*-31). Sodium hydride (60%, 2 g, ca. 50 mmol) was added under nitrogen atmosphere to THF (125 mL) while stirring. The suspension was cooled to 0 °C for 10 min and 2,4-pentanedione (5 g, 50 mmol) was added drop-wise over ca. 3 min. A slightly exothermic reaction took place, resulting in some gas evolution and a thick white suspension was obtained. nBuLi (19 mL, 2.5 M in hexanes) was added in ca. 15 sec with a plastic syringe. A slightly yellow, clear solution was obtained. After 20 min geranyl bromide (7.3 g, 33.62 mmol) was added. The resulting suspension was stirred while warming to RT for 1h. The reaction mixture was quenched with sat. aq. NH_4Cl (70 mL). Extraction with TBME (2 x 150 mL), drying of the organic fractions with Na_2SO_4 and concentration under vacuum gave the crude product (9.66 g, >100%). Purification of a small

sample by ISCO chromatography gave 63 mg pure (E)-8,12-dimethyltrideca-7,11-diene-2,4-dione (GGA*-31) as an oil.

^{1}H-NMR ($CDCl_3$, in ppm): 1.70 (s, 3H), 1.72 (s, 3H), 1.77 (s, 3H), 2.01 (m, 9H), 2.35 (m, 2H), 3.59 (s, 2H), 5.10 (m, 2H), GC-MS: $(M)^+$ = 236,2

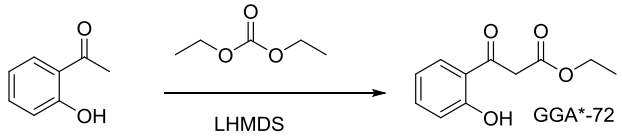

Ethyl 3-(2-hydroxyphenyl)-3-oxopropanoate (GGA*-72). A solution of LHMDS (1M, 220 mL, 220 mmol, 3.0 eq) was under N_2-atmosphere cooled to –78 °C. A solution of 2'-hydroxyacetophenone (8.84 mL, 73.5 mmol, 1.0 eq) in THF (300 mL) was added drop-wise in 30 min. The temperature was maintained at -78 °C for 1 h and 2 h at -10 °C. The solution was cooled again to -78 °C and subsequently a solution of diethylcarbonate (9.8 mL, 80.8 mmol 1.1 eq) in THF (30 mL) was added. The reaction mixture was allowed to warm to RT over the weekend and poured in a mixture of HCl (37%, 50 mL) and ice (1.5 L). The layers were separated and the water layer was extracted with DCM (2 x 500 mL). The combined organic layers were washed with brine (1 x 0.5 L), dried over Na_2SO_4 and concentrated *in vacuo* yielding a yellow oil (16.4 g). The crude product was stirred in DCM and the solids formed were removed by filtration. The filtrate was purified by automated column chromatography (eluens, 0 to 30% EtOAc in heptanes) affording a colorless oil (11.6 g, 55.6 mmol, 76%).

^{1}H-NMR ($CDCl_3$, in ppm): 1.29 (t, 3H), 4, 01 (s, 2H), 4.23 (q, 2H), 6.95 (t, 1H), 7.02 (d, 1H), 7.58 (m, 1H), 7.70 (d, 1H). HPLC-MS: $(M+1)^+$ = 209,2

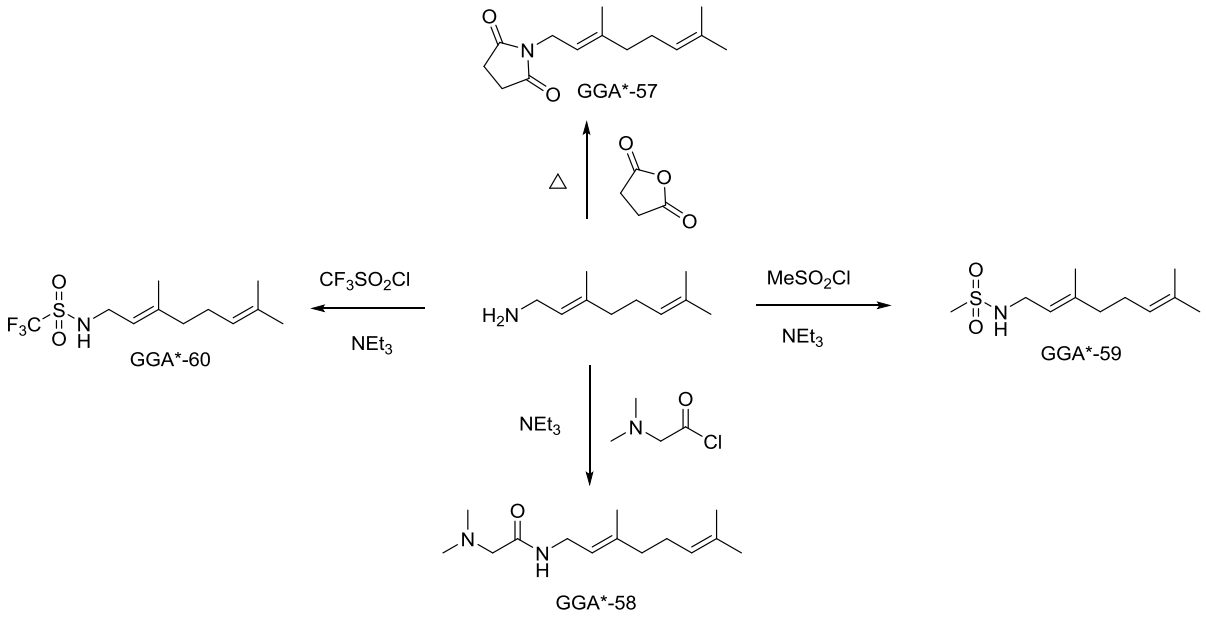

Synthesis of GGA-57, -58, -59 and -60*

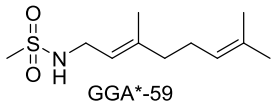

(E)-N-(3,7-Dimethylocta-2,6-dien-1-yl)methanesulfonamide (GGA*-59). A solution of geranylamine (306 mg, 2.0 mmol) and triethylamine (360 mg, 3.6 mmol) in dichloromethane (2 mL) was cooled to 0 ^{o}C with an ice bath and methanesulphonyl chloride (229 mg, 2 mmol) was added. After stirring overnight while warming to RT water (10 mL) was added. Extraction with dichloromethane (2 x 10 mL), drying of the combined organic layers with Na_2SO_4 and concentration under vacuum provided crude GGA*-59. Purification by ISCO chromatography afforded (E)-N-(3,7-dimethylocta-2,6-dien-1-yl)methanesulfonamide GGA*-59 (208 mg, 0,90 mmol, 45%)

^{1}H-NMR ($CDCl_3$, in ppm): 1.60 (s, 3H), 1.68 (s, 3H), 1.70 (s, 3H), 2.05 (m, 4H), 2.99 (s, 3H), 3.79 (t, 2H), 5.10 (m, 1H), 5.22 (m, 1H). HPLC-MS: $(M+1)^+$ = 231.2

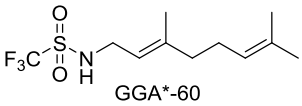

GGA*-60

(E)-N-(3,7-Dimethylocta-2,6-dien-1-yl)-1,1,1-trifluoromethanesulfonamide (GGA*-60). Geranylamine (0.50 g, 3.26 mmol, 1.0 eq) was dissolved in DCM (20 mL) and cooled in a NaCl/ice bath. Triethylamine (0.82 mL, 0.59 g, 5.87 mmol, 1.8 eq) was added and the solution cooled to -13°C. Trifluoromethanesulfonic acid (0.55 mL, 0.920 g, 1.0 eq) was carefully added dropwise in 15 min, keeping internal temperature below -10°C, addition was very exothermic. The reaction mixture was stirred between -15 and -11°C for 30 min, then warmed to 0°C and stirred at that temperature for 1 hour. Water (40 mL) and DCM were added (10 mL), the layers were mixed and separated, and the aqueous phase was extracted with DCM (2x 20 mL). The organic layers were combined, dried with sodium sulfate, filtered and concentrated *in vacuo* to afford a yellow oil (1.02 g) which was purified by ISCO chromatography (Silica, 10% EtOAc/Heptanes) yielding 223 mg (24%) of GGA*-60

^{1}H-NMR ($CDCl_3$, in ppm): 1.60 (s, 3H), 1.68 (s, 6H), 2.07 (m, 4H), 3.92 (m, 2H), 5.05 (m, 1H), 5.22 (m, 1H). HPLC-MS: $(M-1)^+$ = 284,20

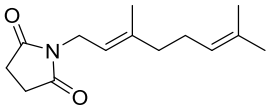

GGA*-57

(E)-1-(3,7-Dimethylocta-2,6-dien-1-yl)pyrrolidine-2,5-dione (GGA*-57). A mixture of geranylamine (300 mg, 2.0 mmol) and succinic anhydride (200 mg, 2 mmol) in dichloromethane (2 mL) was heated with a heating gun for 5 min. The reaction mixture was concentrated *in vacuo*. Purification by ISCO chromatography afforded GGA*-57 (47 mg, 0,20 mmol, 10%).

^{1}H-NMR ($CDCl_3$, in ppm): 1.58 (s, 3H), 1.65 (s, 3H), 1,78 (s, 3H), 2.01 (m, 4H), 2.70 (s, 4H), 4.09 (d, 2H), 5.03 (m, 1H), 5.17 (m, 1H). GC-MS: $(M)^+$ = 235.2

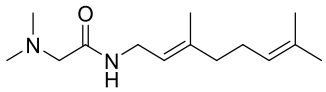

GGA*-58

(E)-2-(Dimethylamino)-N-(3,7-dimethylocta-2,6-dien-1-yl)acetamide (GGA*-58). A solution of geranylamine (311 mg, 2.03 mmol) and triethylamine (360 mg, 3.6 mmol) in dichloromethane (2 mL) was treated with N,N-dimethylaminoacetyl chloride hydrochloride salt (360 mg, 2.3 mmol) at RT. After stirring overnight at RT water (10 mL) was added. Extraction with dichloromethane (2 x 10 mL), drying of the combined organic layers with Na_2SO_4 and concentration under vacuum furnished crude GGA*-58. Purification by ISCO chromatography afforded (E)-2-(dimethylamino)-N-(3,7-dimethylocta-2,6-dien-1-yl)acetamide GGA*-58 (153 mg, 0,64 mmol, 32%).

^{1}H-NMR ($CDCl_3$, in ppm): 1.61 (s, 3H), 1.75 (s, 6H), 2.04 (m, 4H), 2.31 (s, 6H), 2.97 (s, 2H), 3.95 (t, 2H), 5.08 (m, 1H), 5.21 (m, 1H). GC-MS: $(M)^+$ = 238.2

For all compounds LogP was calculated with ChemDraw.

Figures

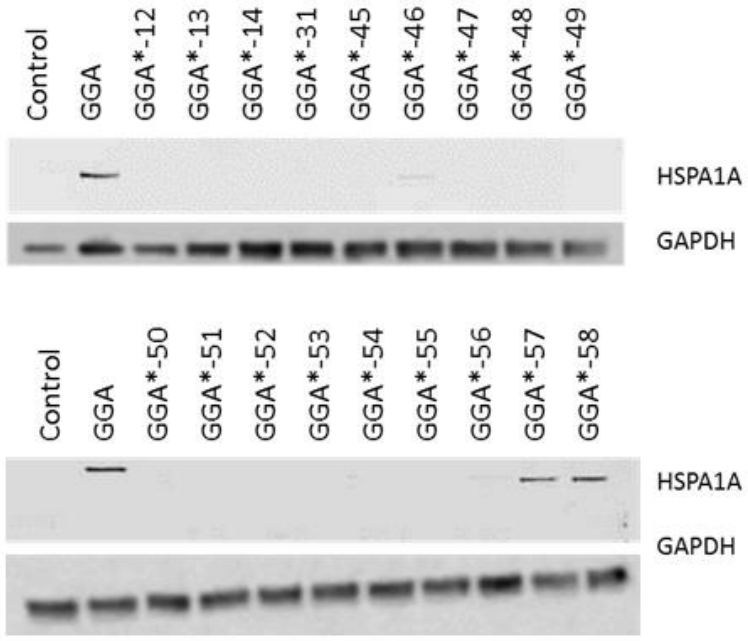

Figure S1. Treatment with GGA and GGA-derivatives gives minor induction of HSPA1A expression in HL-1 cardiomyocytes

HL-1 cardiomyocytes pre-treatment with 10 µM GGA and GGA-derivatives for 6 h reveal minor effect on HSPA1A protein expression.

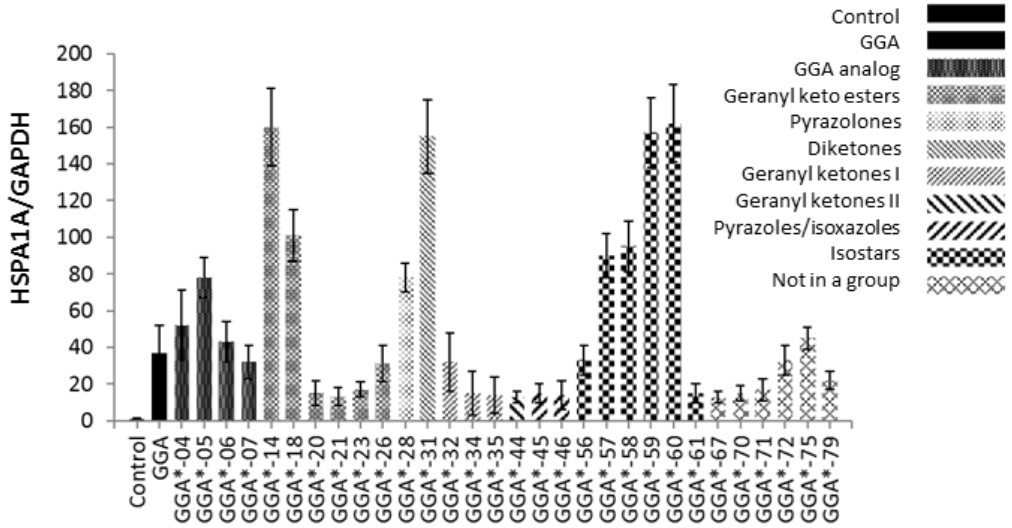

Figure S2. HSPA1A inducing effects of GGA-derivatives cannot be related to groups of same molecular structure.

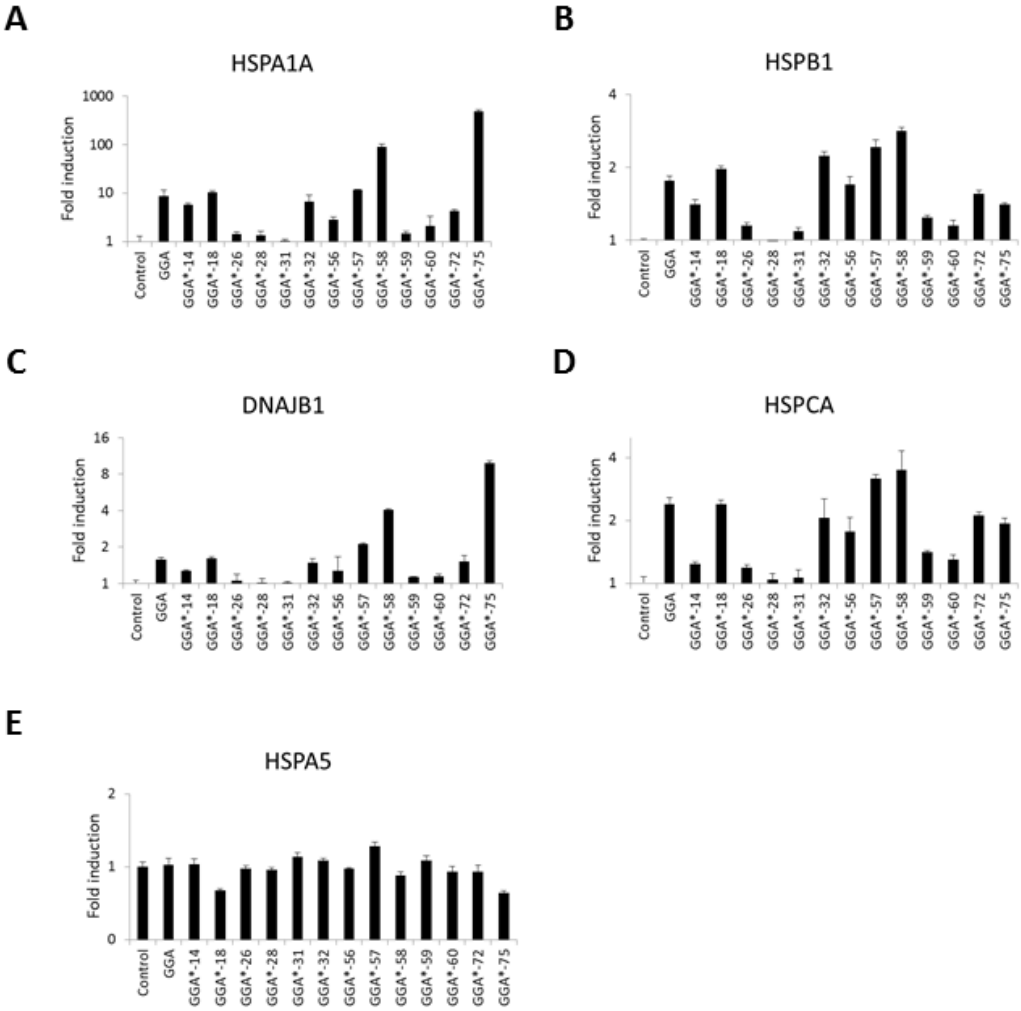

F**igure S3.** GGA-derivatives induce *HSPA1A* (**A**), *HSPB1* (**B**), *DNAJB1* (**C**) and *HSPCA* (log scale) (**D**), but not *HSPA5* (linear scale, not HSF-1 mediated) (**E**) mRNA expression in heat shocked HL-1 cardiomyocytes compared to non-treated heat shocked control HL-1 cardiomyocytes.

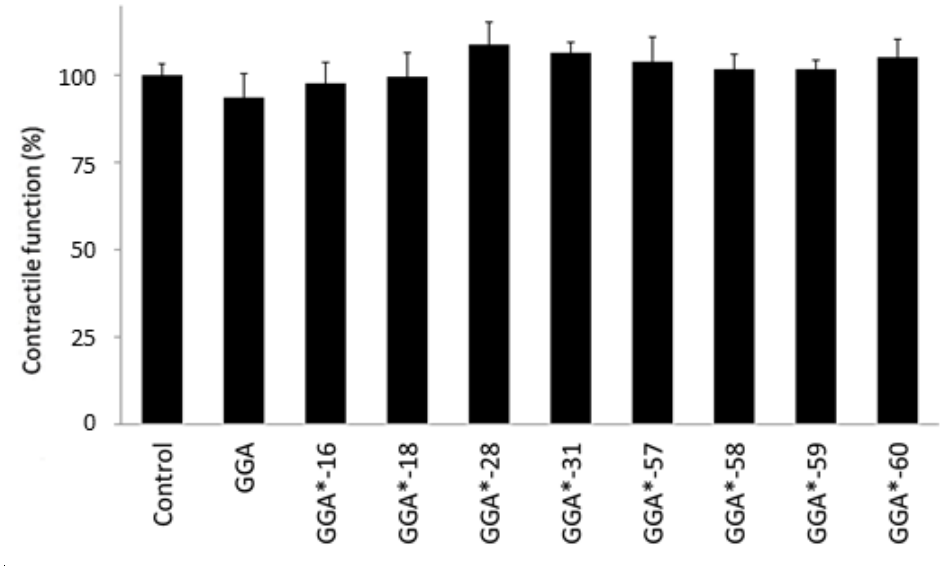

Figure S4 GGA or GGA-derivatives do not affect basal heart rate in *Drosophila* prepupae.

Video S1 Beating heart wall of non-paced control *Drosophila* prepupa (online).

Video S2 Beating heart wall of tachypaced control *Drosophila* prepupa (online).

Video S3 Beating heart wall of non-paced *Drosophila* prepupa pretreated with GGA*-59 (online).

Video S4 Beating heart wall of tachypaced *Drosophila* prepupa pretreated with GGA*-59 (same prepupa as S3, but different part of the body to view heart wall) (online).